大阪大学 CSRN 2018 年度報告会
CSRN-Osaka Annual Workshop 2018

Date: Thu 13 Dec, 2018 - Sat 15 Dec, 2018
Place: Nambu Yoichiro Hall, Graduate School of Science, Osaka University

Organization
Conference Chair: Yoshishige Suzuki
Co-Chair: Tamio Oguchi (International Joint Research Promotion Program (TypeB: Japan-Sweden)), Kazunori Sato (International Joint Research Promotion Program (Type B: Japan-Austria))
Organizing Committee: Kohei Hamaya, Akira Oiwa, Kensuke Kobayashi, Akira Masago, Tetsuya Fukushima
Local Organizing Committee: Akira Masago, Yumi Oda, Aya Honke, Yukimi Murata, Hikari Shinya (Yokohama National University)

Sponsors
Center for Spintronics Research Network (CSRN)
Spintronics Research Network of Japan
International Joint Research Promotion Program (Type B: Japan-Sweden)
International Joint Research Promotion Program (Type B: Japan-Austria)

Map

Cafeteria, canteen(生協食堂 coop-restaurant), ATM(SMBC), and postal office are in the campus. In canteens, only people who have purchased a coop membership are eligible for the member pricing, and hence, non-coop-members have to pay comparatively expensive charges there. In the cafeteria "Laforet", all people pay identical charges regardless of coop membership or not.

食堂・生協食堂・ATM（三井住友）・郵便局がキャンパス内にあります。生協食堂では会員証を提示されない方は一般価格での提供となっています。カフェテリア（らふぉれ, Laforet）は、生協ではないのでそのような価格の違いはありません。図書館下食堂（右上）および食堂（らふぉれ・下）は土曜日も営業しております。また正門の外側の正面にファミリーレストランがあります。

Internet access

Only eduroam is available.

Usage of Nambu Hall

No smoking in this Hall. No food, drink, and plastic bottles in this Hall including the session area. In the communication salon, it is possible to have and drink.

建物内は禁煙です。セッションエリアを含むホール内は飲食禁止です（ペットボトルも不可）。交流サロンのテーブル・椅子は、飲食を伴う懇親会等に使用できます。

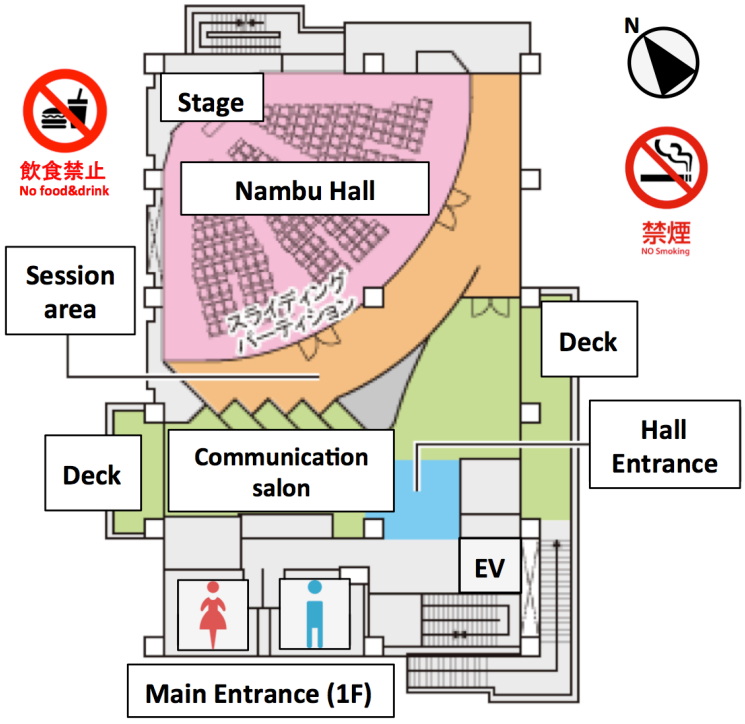

Program

Date: Thu 13 Dec, 2018 - Sat 15 Dec, 2018
Place: Nambu Yoichiro Hall, Graduate School of Science, Osaka University
Regulation: 20min Talk, 5min Discussion, 5min Interval; Japanese/English
All speakers are invited.

Thu 13 Dec		
09:30		Registration
10:20		Opening remarks: Y. Suzuki (Osaka Univ)
Session A: Semiconducting Spintronics (Chair: A. Masago)		
10:30		Y. Niimi (Osaka Univ)
11:00		M. Yamada (Osaka Univ)
11:30	13:30	Lunch and Poster Session (box-lunch provided)
Plenary Session I (Chair: T. Oguchi)		
13:30		O. Eriksson (Uppsala Univ, Sweden)
Session B: Semiconducting Spintronics (Chiar: T. Oguchi)		
14:00		S. Kuroda (Univ of Tsukuba)
14:30		H. Tanaka (Osaka Univ)
15:00		Break
Session C: Quantum Computing (Chair: H. Katayama-Yoshida)		
15:30		Y. Utsumi (Mie Univ)
16:00		M. Negoro (Osaka Univ)
16:30		A. Oiwa (Osaka Univ)
17:00		Photo
18:30	20:30	Banquet (Ganko, Ishibashi)
Fri 14 Dec		
08:30		Registration
Session D: Metallic Spintronics (Chair: Y. Suzuki)		
09:00		C. Hwang (Korean research institute of standards and science, Korea)
09:30		H. Nomura (Osaka Univ)
10:00		M. Goto (Osaka Univ)
10:30		Y. Kurokawa (Kyushu Univ)
11:00		T. Kimura (Kyushu Univ)
11:30		Lunch
14:50	16:10	Excursion (Yamazaki Distillery)

Sat 15 Dec

08:30	Registration

Plenary Session II (Chair: K. Sato)

09:00	A. Bonanni (Johannes Kepler Univ, Austria)

Session E: Theory and Simulations (Chair: K. Sato)

09:30	H. Okumura (Osaka Univ)
10:00	T. Yamashita (NIMS)
10:30	N. Hamada (Osaka Univ)
11:00	B. Sanyal (Uppsala Univ, Sweden)
11:30	Closing T. Oguchi (Osaka Univ)

Lunch:
Packed-lunch will be provided only on Thursday, December 13.
Cafeterias are available during the Workshop.

Banquet:
Place: Ganko Ishibashi
URL: https://www.gankofood.co.jp/en/
Date: 18:30-20:30, Thursday, December 13
Directions: five-minute walk from Handai-Sakashita.
Meeting point: Ganko Ishibashi
We have chartered a micro bus for Senri Hankyu Hotel.

Excursion:
Place: Suntory whisky Yamazaki Distillery (capacity of 21 persons)
URL: https://www.suntory.com/factory/yamazaki/
Date: 14:50-16:10, Friday, December 14
Meeting point: Gate of Suntory Whisky Yamazaki Distillery
Directions:
ten-minute walk from Hankyu Oyamazaki station.
ten-minute walk from JR Yamazaki station.
forty-one-minute from Osaka-Monorail Shibahara station to Hankyu Oyamazaki station (change lines at Minami-Ibaraki station)

Abstracts for oral presentations

Abstracts for poster presentations

Abstracts for oral presentations

No. A1

Application of 2D antiferromagnetic materials to spintronic devices

H. Taniguchi[1], S. Suzuki[1], T. Kawakami[1], T. Arakawa[1,2], H. Yoshida[3],
S. Miyasaka[1], S. Tajima[1], K. Kobayashi[1,2], and Y. Niimi[1,2*]

[1]*Graduate School of Science, Osaka University, Osaka, Japan*

[2]*Center for Spintronics Research Network, Osaka University, Osaka, Japan*

[3]*Graduate School of Science, Hokkaido University, Hokkaido, Japan*

Email: niimi@phys.sci.osaka-u.ac.jp

Graphene, a single atomic layer of graphite, is a pioneering two-dimensional (2D) material. In the field of spintronics, graphene has been used as a transporter of spin current in the lateral spin valve [1] because of its long spin diffusion length. Recently, 2D ferromagnetic materials have been reported [2], which can be integrated in future atomic-layer spintronic devices. The motivation of the present study is to find out conductive 2D antiferromagnets and fabricate spintronic devices with them.

Ag_2CrO_2 is one of the conductive triangular antiferromagnets with the transition temperature T_N of 24 K [3]. The Cr site has the spin angular momentum of 3/2 and is arranged on a triangular shape, while the Ag_2 layer is in charge of the electrical conductivity (see Fig. 1(a)). According to a theoretical calculation on 2D triangular antiferromaget [4], a unique thermodynamic state, the so-called partially-disordered (PD) state, appears at finite temperatures. However, the detailed magnetic structure of the PD state is still unclear because the single crystal has not been prepared yet. Recently, we have developed a new method to obtain higher quality thin films of Ag_2CrO_2 from the polycrystalline samples [5] and performed magnetotransport measurements. The magnetoresistance shows a typical spin-valve behavior only in the vicinity of T_N, which should be definitely related to the PD spins.

High critical-temperature (T_C) superconductors are also based on the 2D antiferromagnetic structure. The host material has the antiferromagnetic ordering and is inherently insulating, but by doping some elements, it shows the superconductivity at relatively high temperatures. We are now aiming to integrate high-T_C superconductors into spintronic devices. For this purpose, we have established the methods to obtain the electrical contact to a thin layer of $Bi_2Sr_2CaCu_2O_{8+\delta}$ (Bi2212) [6] and also to superimpose graphene on top of the Bi2212 film.

[1] N. Tombros *et al*., Nature **448**, 571 (2007).
[2] C. Gong *et al*., Nature **546**, 265 (2017).
[3] H. Yoshida *et al*., J. Phys. Soc. Jpn. **80**, 123703 (2011).
[4] T. Takagi and M. Mekata, J. Phys. Soc. Jpn. **64**, 4609 (1995).
[5] H. Taniguchi *et al*., AIP Adv. **8**, 025010 (2018).
[6] S. Suzuki *et al*., Appl. Phys. Express **11**, 053201 (2018).

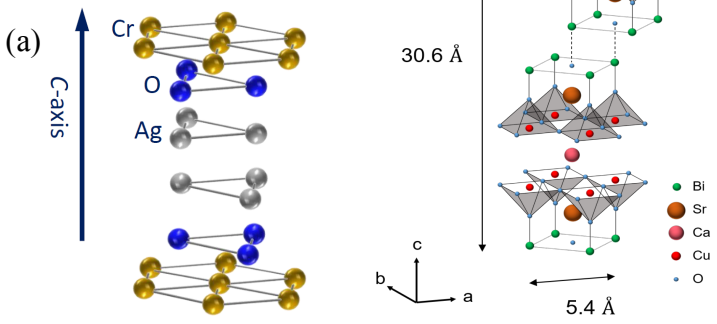

Fig.1 : Crystal structures of (a) Ag_2CrO_2 and (b)

No. A2

Spin transport in Ge and SiGe

M. Yamada[1,2], M. Tsukahara[1], Y. Fujita[1], T. Naito[1], S. Yamada[1,3],
K. Sawano[4], and K. Hamaya[1,3]

[1] *Graduate School of Engineering Science, Osaka University, Osaka 560-8531, Japan,*
[2] *JSPS Research Fellow, Tokyo 102-0083, Japan*
[3] *Center for Spintronics Research Network, Osaka University, Osaka 560-8531, Japan*
[4] *Advanced Research Laboratories, Tokyo City University, Tokyo 158-0082, Japan*
E-mail: michihiro@ee.es.osaka-u.ac.jp

For semiconductor spintronic devices, it is important to understand spin transport and relaxation in the channel layers. Recently, we observed spin transport in *n*-Ge up to room temperature, and discussed the spin relaxation mechanism [1,2]. Here we report reliable spin transport data in *n*-Ge and *n*-$Si_{0.1}Ge_{0.9}$ layers at around room temperature.

Lateral spin valve (LSV) devices were fabricated by conventional electron-lithography and Ar^+ milling, as shown in Fig. 1(a). For spin injection and detection, $Co_2FeAl_xSi_{1-x}$/*n*-Ge or $Co_2FeAl_xSi_{1-x}$/*n*-$Si_{0.1}Ge_{0.9}$ Schottky tunnel contacts were used. The size of the contacts is 0.4 × 5.0 μm^2 and 1.0 × 5.0 μm^2, respectively.

We measured four-terminal nonlocal (NL) magnetoresistance and Hanle-effect curves at around room temperature. For *n*-Ge, clear NL spin signals and Hanle curves can be seen in the inset of Fig. 1(b) and Fig. 1(c), meaning reliable room-temperature spin transport. From the dependence of the NL spin signal on the distance (*d*) between injector and detector and Hanle curves, the spin diffusion length at room temperature can be estimated to be ~ 0.44 μm [2]. We will talk about the data for *n*-$Si_{0.1}Ge_{0.9}$ [3].

This work is partly supported by MEXT/JSPS KAKENHI (Grant No. 16H02333, 17H06832, 17H06120, 18J00502, and 26103003).

References

[1] Y. Fujita *et al.*, Phys. Rev. Applied **8**, 014007 (2017).
[2] M. Yamada *et al.*, Appl. Phys. Express **10**, 093001 (2017).
[3] T. Naito *et al.*, Appl. Phys. Express **11**, 053006 (2018).; M. Yamada *et al.*, Semicond. Sci. Technol. **33**, 114009 (2018).

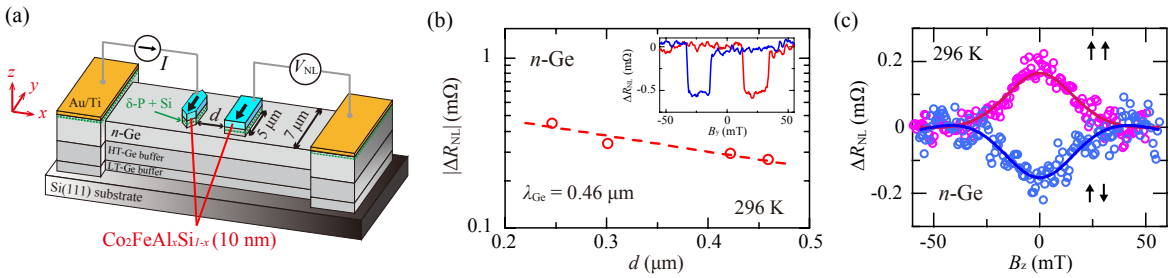

Fig. 1 (a) Schematic illustration of fabricated lateral spin valve device. (b) *d* dependence of nonlocal spin signal at 296 K. Inset shows a nonlocal magnetoresistance curve at 296 K. (c) Four-terminal nnonlocal Hanle-effect curves under parallel and anti-parallel magnetization states at 296 K.

No. B1

Optical detection and manipulation of a single Cr spin in a semiconductor quantum dot

A. Lafuente-Sampietro[1,2], M. Sunaga[1], K. Makita[1], M. Arino[1],
H. Boukari[2], L. Besombes[2], and S. Kuroda[1,3]

[1] *Institute of Materials Science, University of Tsukuba, Tsukuba, 305.8573, Japan*

[2] *Université Grenoble Alpes, CNRS, Institut Néel, 38000 Grenoble, France*

[3] *Center for Spintronics Research Network, Osaka University, Toyonaka, 560-8531, Japan*

Email: kuroda@ims.tsukuba.ac.jp

Control of a single spin has been attracting attention from the viewpoint of both basic physics and application for quantum information technology. Among various systems of a single spin studied so far, we have been focusing on the spin of a single atom of transition-metal (TM) elements confined in semiconductor quantum dots[1-3]. The incorporation of Cr in II-VI compounds is of particular interest because of a finite orbital angular moment $L = 2$ of a Cr^{2+} ion substituting the cation site which provides a strong coupling with lattice strain[4]. In this case, the spin-orbit interaction connects the Cr spin to the local strain environment through the modification of crystal field splitting, which raises an expectation of realizing spin-mechanical coupling system.

In the present study, we fabricate self-assembled dots (SAD) of CdTe containing a single Cr atom in the hetero-epitaxy on ZnTe (001) surface by molecular beam epitaxy. The photoluminescence (PL) spectrum from an exciton confined in the single-Cr dot is split into several lines as shown in Fig. 1, due to the exchange interaction with the Cr spin. The five-fold degeneracy of the total spin momentum $S = 2$ state of Cr^{2+} is lifted due to an in-plane strain inside SADs, resulting in the emission only from the states with the z-component $S_z = \pm 1, 0$[4]. Additional lines appear due to the splitting caused by the anti-crossing behaviors and the emission from the dark exciton state[4].

We investigate the energy configuration and dynamics of the Cr spin states by various optical measurement techniques such as magneto-optics[4], auto correlation[5] and pump-probe measurements[6]. In the pump-probe measurement, we prepare the specific Cr spin state by resonantly exciting one of the lines and probe its relaxation by observing the emission of another line (optical pumping). As shown in Fig. 2, we reveal the relaxation of Cr spin is relatively slow around 2μs in the dark in contrast to the fast relaxation of the order of tens nanoseconds in the presence of an exciton, which is attributed to the flip-flop process of the hole and Cr spin[7].

References

[1] L. Besombes *et al.*, Phys. Rev. Lett. **93**, 207403 (2004). [2] J. Kobak *et al.*, Nat. Commun. **5**, 3191 (2014). [3] T. Smoleński *et al.*, Nat. Commun. **7**, 10484 (2016). [4] A.

Lafuente-Sampietro *et al.*, Phys. Rev. B **93**, 161301(R) (2016). [5] A. Lafuente-Sampietro *et al.*, Appl. Phys. Lett. **109**, 053103 (2016). [6] A. Lafuente-Sampietro *et al.*, Phys. Rev. B. **95**, 035303 (2017). [7] A. Lafuente-Sampietro *et al.*, Phys. Rev. B **97**, 155301 (2018).

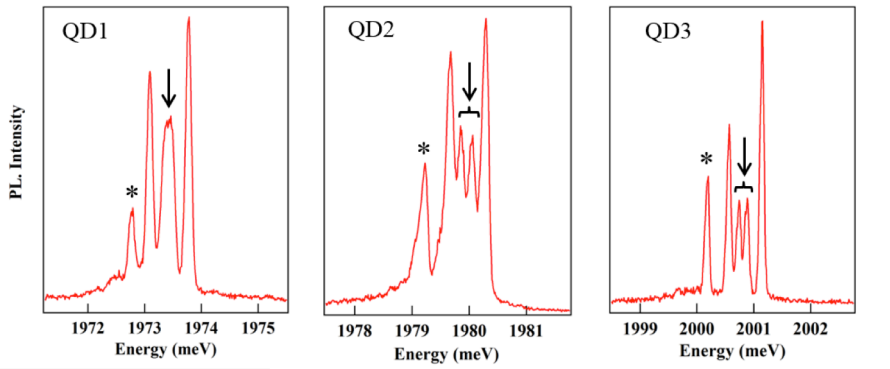

Figure 1: Typical examples of the emission spectra from the single-Cr dot. The central emission line is split into two lines due to the anti-crossing behavior (denote by arrows in QD2, 3), and an additional line from the dark exciton state appears (denoted by *).

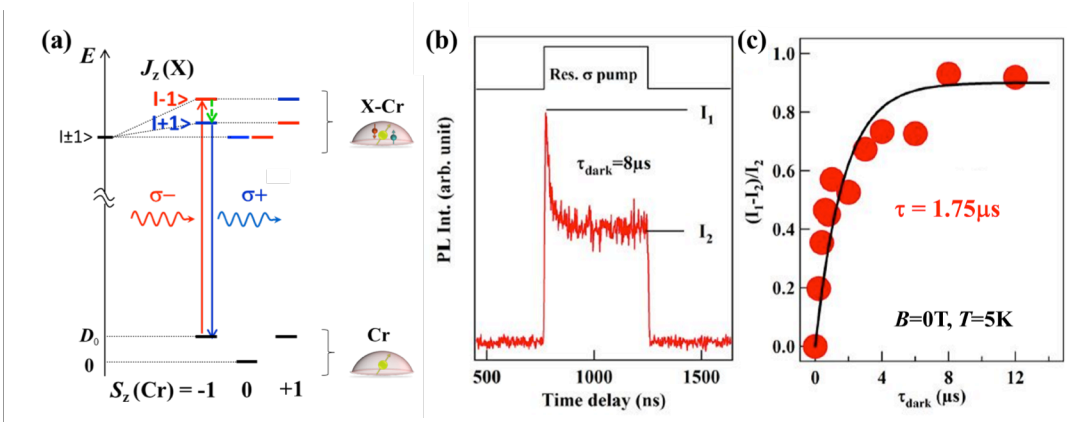

Figure 2: The concept and results of the optical pumping experiment. (a) Energy diagram of the single Cr spin state and the optical transition for the excitation/ detection under resonant optical pumping. (b) Time evolution of PL intensity of the lower-energy line under the resonant excitation of S_z = -1 state with σ⁻ polarization at the higher-energy line. (c) The amplitude of the pumping decay $(I_1 - I_2)/I_2$ as a function of the dark time between the successive pump pulses.

No. B2

Strain driven high-efficiency electronic-phase switching in freestanding transition metal oxide nano/microstructures

Hikdeazu Tanaka[1,2], Teruo Kanki [1,2], L. Pellegrino[3], D. Marre[3, 4]

[1] *Institute of Scientific and Industrial Research, Osaka University*

[2] *Center spintronics research network (CSRN), Osaka University*

[3] *CNR- Superconducting and other innovative materials and devices institute, Italy*

[4] *University of Genova, Italy*

Email: h-tanaka@sanken.osaka-u.ac.jp

Transition metal oxides possess unique functionalities, such as ferromagnetic, and superconductiong properties. Their nanostructures are indispensable to achieve the advanced nanoscale electronic devices [2]. We have been developed a novel nanofabrication techniques by combining epitaxial growth by pulsed laser deposition (PLD) and nanoimprint lithography (NIL) techniques. Using these techniques, metal-insulator transition oxide nanowire and field effect transistor, magnetoresistive oxide nanowall and nano-boxes (manganite), Photo-luminescent nanowall/box array (ZnO), ferromagnetic oxide nano-dots, Free standing oxide NEMS (nano-electro-mechanical system) [3-7] have been fabricated.

Electrostatic-actuation of freestanding membranes, which is widely used in Micro-/Nano-electromechanical system (MEMS/NEMS) actuators, is a promising way for leading the practical applications because of dynamically generating lattice strain through electrostatic attractive forces. We constructed several hundred nanometer-scaled single crystalline freestanding nanowires with planer-type double side-gates and demonstrated modulation of transport properties of VO_2 freestanding nanowires by electrostatic actuation.

Figure 1 shows the scanning electron microscope (SEM) images of VO_2 freestanding nanowires with planer-type double side-gates in a width of 800 nm. From this image, The NEMS structure with hung side-gates and suspended channel parts can be confirmed. In Fig.2, with increasing the V_G in the side gate, namely, magnitude of strain, the insulator to metal transition occurs in local nano domains. In strain-inducing process from initial state, VO_2 maintained insulating state and indicates high resistance.

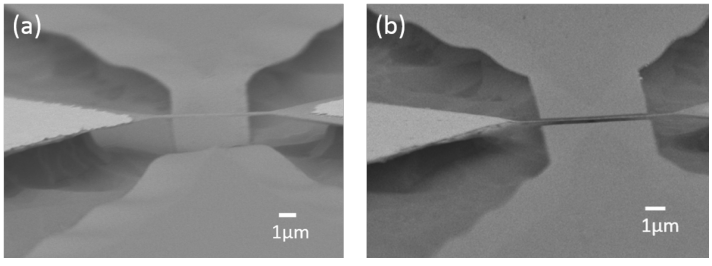

Figure 1 The scanning electron microscopy (SEM) images of freestanding nanowires with two different etching time; (a) 4hours and (b) 2hours.

Eventually, nano-domains change to the metallic phase beyond a barrier between metallic and insulating minimum potentials, which is (i) and (iii) processes. In the strain-releasing process of (ii) and (iv), insulating nano domains turn to metallic states beyond the barrier. Thus, the butterfly shape was appeared due to hysteresis between insulating states and metallic states. Such a hysteretic behavior proves resistance modulation was occurred by metal-insulator transition.

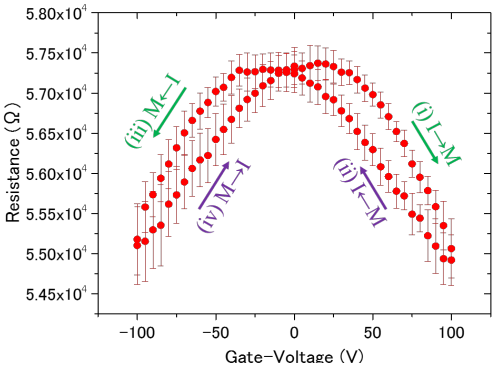

Figure 2: The averaged values of resistance in each gate voltage during the ten cycle measurements of gate-bias dependence of resistance. The error bars indicate their standard deviations.

Figure 3 shows the where R_{VG} and R_{0V} are the resistance during applying the V_G and without V_G, respectively, as a function of temperature and applied gate-bias. The resistance modulation ratio start to increase from 330K to 336 K The ratios are approximately 0.19 % at 330 K and 17.1 % at 336 K at V_G=+200 V, respectively. Thus, the modulation efficiency of the resistance was continued to enhance as elevated to the transition temperature of 339K, where is the maximum point of dR/dT in freestanding nanowires.

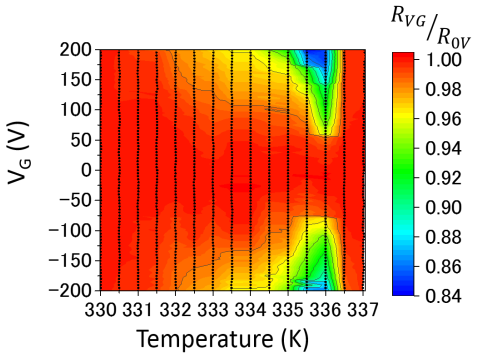

Figure 3: The normalized resistance (R_{VG}/R_{0V}) as a function of temperature (x-axis) and applied gate-bias (y-axis). Temperature step was 0.5K.

This transition metal oxide freestanding nanostructure will provide current /strain induced phase transition such as ferromagnetic to paramagnetic phase transition in magnetic semiconductor, ferromagnetic oxide and so on.

References

1. H. Tanaka, H. Takami, T. Kanki, A. N. Hattori, and K. Fujiwara, Jpn. J. Appl. Phys. 53 (2014) 05FA10
3. Y. Higuchi, T. Kanki and H. Tanaka , Appl. Phys. Exp. 10 (2017) 033201 (1-4)
4. N. Manca, L. Pellegrino, T. Kanki, W. J. Venstra, G. Mattoni, Y. Higuchi, H. Tanaka, A. D. Cavigila, and D. Marre, Adv. Mater. 29 (2017) 1701618
5. N. Manca, T. Kanki, H. Tanaka, D. Marre and L. Pellegrino, Appl. Phys. Lett. 107 (2015) 143509(1-6).
6. S. Yamasaki, T. Kanki, N. Mancla, L. Pellegrino, D. Marre and H. Tanaka, Appl. Phys. Exp. 7 (2014) 023201
7. N. Manca, L. Pellegrino, T. Kanki, S. Yamasaki, H. Tanaka, A. S. Siri and D. Marre Advanced Materials 25 (2013) 6430-6435

No. P1

Applications of Solitonics and Magnonics

O. Eriksson[1,2]

[1] *Department of Physics and Astronomy, Uppsala University, Sweden*

[2] *School of Science and Technology, Örebro University, Sweden*

Email: olle.eriksson@physics.uu.se

This talk covers the basic foundation of spin-dynamics simulations, and how materials specific modeling can be done via a coupling of the atomistic Landau-Lifshitz-Gilbert equation and density functional theory. Examples of how this theory reproduce experimental observations will be presented [1]. Technological possibilities of these simulations will be outlined, in the field of solitonics[2] and magnonics [3], where in the latter the majority gate is demonstrated to operate with chiral magnetic excitations.

References

[1] O.Eriksson, A.Bergman, L.Bergqvist, J.Hellsvik, "Atomistic spin-dynamics; foundations and applications" (Oxford university press, Feb 2017 ISBN 9780198788669).

[2] Konstantinos Koumpouras, Anders Bergman, Olle Eriksson and Dmitry Yudin, Scientific Reports **6**:25685 (2016).

[3] Konstantinos Koumpouras, Dmitry Yudin, Christoph Adelmann, Anders Bergman, Olle Eriksson and Manuel Pereiro, J. Phys. Cond. Matt. **30**, 375801 (2018).

No. C1

Information flow through a mesoscopic quantum device

Y. Utsumi

Department of Physics Engineering, Mie University, Tsu, Mie, 514-8507, Japan

Email: utsumi@phen.mie-u.ac.jp

The laws of physics limit the performance of information processing such as the communication process [1]. The quantum physics also dominates the performance the information transmission through a communication channel. In the information theory, a model communication system consists of a transmitter, a channel, and a receiver [2] [Fig. (a)]. A measure of the performance of the channel is *capacity* C, the maximum possible rate at which information can be transmitted without error. Shannon demonstrated that the information capacity is limited by the average signal power P as $C = B \ln(1 + P/N)$, where B is the bandwidth and N is the noise power [2]. For a quantum communication channel, the optimum capacity is limited by the square root of the signal power $C = (\pi P/3)^{1/2}$ [3]. Although these relevant results have been obtained three decades ago, there are not many works clarifying the connection between the physics of mesosicopic quantum devices and the theory of communication [4].

Here we discuss the information transmission through a mesoscopic quantum conductor, a quantum dot [Fig. (a)]. The optimum capacity is related to the average of self-information J, which is a fluctuating variable. We analyze the fluctuations of the self-information by calculating its probability distribution function $\mathrm{P}(J)$, which contains valuable information about the communication process [5]. We will demonstrate the universal relation connecting the fluctuation and the optimum capacity $\langle \exp(J) \rangle = \exp(\tau C)$. Then we will discuss the bandwidth dependence of the optimum capacity [Fig. (b)]. Technically, we evaluate the order M Rényi entanglement entropy R_M of a bipartite quantum conductor in the non-equilibrium steady state by exploiting the multi-contour Keldysh Green function [6].

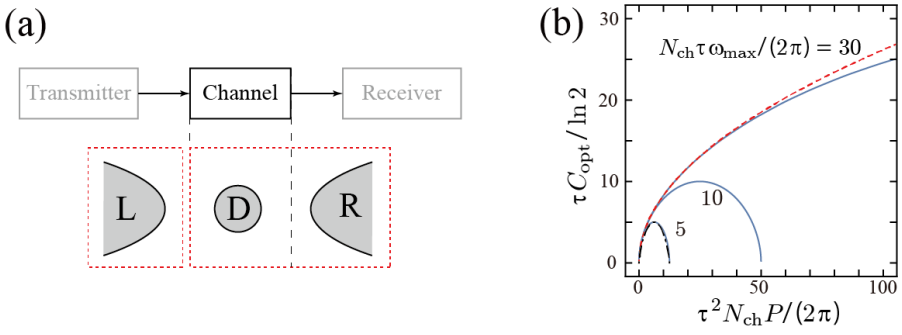

References

[1] R. Landauer, Science, **272**, 1914 (1996); S. Lloyd, Nature, **406**, 1047 (2000).

[2] C. E. Shannon, Bell System Techn. J. **27** 379-423, 623-656 (1948).

[3] J. B. Pendry, J. Math. A: Math. Gen. **16**, 2161 (1983); C. M. Caves and P. D.

Drummond, Rev. Mod. Phys. **66**, 481 (1994); M. P. Blencowe, and V. Vitelli, Phys. Rev. A **62**, 052104 (2000).
[4] U. Sivan and Y. Imry, Phys. Rev, B **33**, 551 (1986); E. Akkermans, Eur. Phys. J. E **28**, 199 (2009).
[5] Y. Utsumi, arXiv:1807.04338.
[6] Yu. V. Nazarov, Phys. Rev. B **84**, 205437 (2011); M. H. Ansari and Yu. V. Nazarov, Phys. Rev. B **91**, 104303 (2015); Y. Utsumi, Phys. Rev. B **92**, 165312 (2015).

No. C2

Abstract title

M. Negoro[1]

[1] *Graduate School of Science, Osaka University, Osaka, Japan*

[2] *Center for Spintronics Research Network, Osaka University, Osaka, Japan*

Email: negoro@ee.es.osaka-u.ac.jp

No. C3

Photon-spin Poincaré interface using electron spins in gate-defined quantum dots

A. Oiwa

[1] *The Institute of Scientific and Industrial Research, Osaka University, Osaka, Japan*

[2] *Center for Spintronics Research Network (CSRN), Graduate School of Engineering Science, Osaka University, Osaka, Japan*

[3] *Quantum Information and Quantum Biology Division, Institute for Open and Transdisciplinary Research Initiatives, Osaka University, Osaka, Japan*

Email: oiwa@sanken.osaka-u.ac.jp

We study the quantum interface (Poincaré interface) based on quantum state conversion using electron spins in gate-defined quantum dots (QDs) for long distance quantum communication [1]. The technical challenges towards this goal for photons and electron spin in the gate-defined QDs are the quantum state conversion from single photons to single electron spins and the entanglement conversion from photon pairs to electron spin pairs. It has been demonstrated that angular momentum of single photons can be converted to single electron spins in gate-defined double QDs [2].

In this talk, we present the quantum state conversion in a gate-defined QD and the coincidence measurement between single photo-electron detection in a QD and single photon detection using an entangled photon source [3]. Moreover the recent progresses on the enhancement of the coupling between photons and electron spins in QDs are discussed.

References

[1] A. Oiwa et al., J. Phys. Soc. Jpn. **86**, 011008 (2017).

[2] T. Fujita et al., arXiv:1504. 03696.

[3] K. Kuroyama et al., Sci. Rep. **7**, 16968 (2017).

No. D1

Structure and motion of in-plane skyrmion

K.-W. Moon, J. Yoon, C. Kim, and Chanyong Hwang

Spin Convergence Research Team, Korea Research Institute of Standards and Science, Daejeon, Korea

Email: cyhwang@kriss.re.kr

Recently, understanding the topological phenomena has been an important issue even in magnetism. Finding the topologically non-trivial spin structure in magnetism becomes very important for its possible application in spintronics. Among topological spin textures, skyrmion is one of the most studied examples. However, most of these studies have been confined in perpendicularly magnetized system. In my talk, we will introduce new type of skyrmions especially in the magnetic system with in-plane magnetic anisotropy. Its structure and motion under the current flow will be introduced[1].

References

[1] K.-W. Moon et al., submitted

No. D2

Reservoir computing with nanomagnets array

Hikaru Nomura[1], Ferdinand Peper[2] , Kazuki Tsujimoto[1], Yuki Kuwabiraki[1], Taishi Furuta[3], Eiiti Tamura[3], Shinji Miwa[3,4,5], Minori Goto[3,4], Yoshishige Suzuki[3,4] and Ryoichi Nakatani[1]

[1]*Graduate School of Engineering, Osaka University, Suita, Osaka, JAPAN*

[2] *Center for Information and Neural Networks,*
National Institute of Information and Communications Technology,
Osaka University, Suita, Osaka 565-0871, Japan

[3]*Graduate School of Engineering Science, Osaka University, Suita, Osaka, JAPAN*

[4]*Center for Spintronics Research Network,*
Osaka University, Toyonaka, Osaka 560-8531, Japan

[5] *The Institute for Solid State Physics,*
The University of Tokyo, Kashiwa Chiba 277-8581, Japan

Email: nomura@mat.eng.osaka-u.ac.jp

Recurrent neural network (RNN)[1] is one of the most promising devices for an artificial intelligent. In RNNs, information is calculated and stored in nodes with closed feedback loops. RNNs show excellent performance to solve multiple tasks such as voice recognition, game of Go, etc. However, an energy consumption of a computer based RNN is increasing associate with improvement of a RNN performance. To reduce the energy consumption, a reservoir computing have been introduced. In reservoir computing, the feedback loops between the nodes can be replaced with a physical phenomenon. [2-4].

In this study we demonstrate a reservoir computing with nanomagnets array with macrospin simulations[5]. The nanomagnets reservoir is composed of 20 nanomagnets. A reservoir state is defined as a direction of static magnetization of the nanomagnets. To update the reservoir state, we change uniaxial anisotropies of the nanomagnets. To check a performance of the reservoir computing, we use binary task of AND, OR and XOR functions. As a result, the reservoir computing can be trained to perform the AND, OR and XOR tasks with up to an input delay of three steps. We expect that devices derived from NM-NN will be widely used as neural network hardware based on spintronics in the near future. This research and development work was supported by the Ministry of Internal Affairs and Communications, Japan.

[1] H. T. Siegelmann and E. D. Sontag, Applied Mathematics Letters 4 (1991), pp. 77–80.

[2] K. Vandoorne, et al., Nature Communications 5 (2014).

[3] K. Nakajima, H. Hauser, T. Li and R. Pfeifer, Scientific Reports 5 (2015).

[4] J. Torrejon, et al., Nature 547 (2017) (7664), pp. 428–431.

[5] H. Nomura, et al., arXiv: 1810.13140

No. D3

Heat driven microwave amplification in magnetic tunnel junction with double MgO layer

M. Goto[1,3], Y. Wakatake[1], U. K. Oji[1], S. Miwa[1,3], N. Strelkov[4,5], B. Dieny[4], H. Kubota[2], K. Yakushiji[2], A. Fukushima[2], S. Yuasa[2], and Y. Suzuki[1,3]

[1] *Graduate School of Engineering Science, Osaka University, Osaka, Japan*

[2] *National Institute of Advanced Industrial Science and Technology (AIST), Ibaraki, Japan*

[3] *Center for Spintronics Research network (CSRN), Graduate School of Engineering Science, Osaka University, Osaka, Japan*

[4] *Grenoble Alpes University, CEA, CNRS, Grenoble INP, INAC, SPINTEC, 38000 Grenoble, France*

[5] *Department of Physics, Moscow Lomonosov State University, Moscow 119991, Russia*

Email: goto@mp.es.osaka-u.ac.jp

Fast and giant spin-torque is required for developing microwave devices in spintronics. The magnetic anisotropy change by Joule heating is one of the promising techniques for spin control. Recently, Böhnert et al. reported that MgO thin film has lower thermal conductivity than bulk one [1]. The ferromagnetic free layer between adjacent MgO layers is efficiently heated by suppression of heat dissipation.

We have investigated the anisotropy change of FeB free layer between the adjacent MgO layers as thermal insulators. The sample, buffer layer | CoFeB(2) reference layer | MgO(1.1) | FeB(1.7) free layer | MgO(1.0) | cap layer, was deposited on thermally oxidized Si substrate (nm in thickness). Figure 1 shows the bias-voltage dependence of the magnetic anisotropy energy measured by the spin-torque diode effect. The parabolic voltage dependence of anisotropy energy was observed, which is attributed to the Joule heating. We found that the magnitude of voltage induced magnetic anisotropy change is up to 300 fJ/Vm. We also demonstrate the microwave amplification driven by heat-driven anisotropy change. We have obtained the amplification gain of more than 20% [2].

This research was supported by Bilateral Programs (MEXT), MIC, ImPACT program of the Council for Science, Technology, and Innovation (Cabinet Office, Government of Japan), and JSPS KAKENHI (Grant No. JP16H03850).

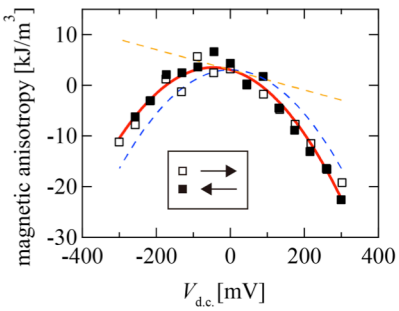

Fig. 1 Voltage dependence of magnetic anisotropy energy

References

[1] T. Böhnert *et al.*, Phys. Rev. B, **95**, 104441 (2017)

[2] M. Goto *et al.*, Nat. Nanotechnol, *accepted.*

No. D4

Current-induced domain wall motion in rare-earth transition-metal alloy magnetic wire for future memory

Yuichiro Kurokawa[1], Masakazu Wakae[1], Satoshi Sumi[2], Hiroyuki Awano[2], and Hiromi Yuasa[1]

[1] *Graduate School and Faculty of Information Science and Electrical Engineering, Kyushu University, 744 Motooka, Nishi-ku, Fukuoka, 819-0395, Japan*

[2] *Information Storage Materials Laboratory, Toyota Technological Institute, 2-12-1 Hisakata, Tenpaku-ku, Nagoya 468-8511, Japan*

Email: ykurokawa@ed.kyushu-u.ac.jp

Manipulating magnetic domain wall (DW) using electric current has attracted significant attention from the viewpoint of device application such as new types of magnetic memories and logic [1,2]. In particular, race track memory suggested by IBM is novel data storage using current induced domain wall motion (CIDWM), and it has potential as a future memory [1]. A number of experimental investigations for the CIDWM have been carried out. However, the threshold current density (J_{th}) for the CIDWM is still high. In this study, we investigate the CIDWM in amorphous rare-earth transition-metal magnetic alloys to obtain low J_{th}. The amorphous rare-earth transition-metal magnetic alloys, for example Tb-Co and Gd-Fe, are ferrimagnetic material with low saturation magnetization (M_s). We expected that the J_{th} in the amorphous rare-earth transition-metal magnetic alloy can be low because it proportional to M_s.

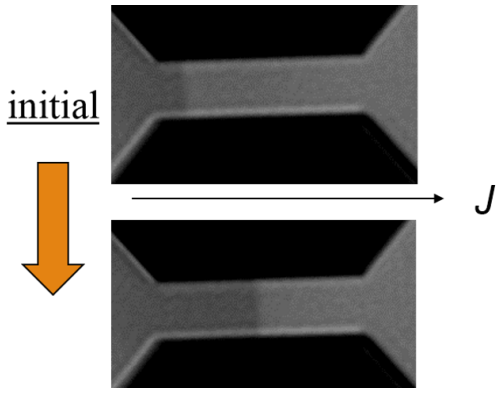

Fig. 1 Kerr image of Gd-Fe alloy wire under electric current (J)

Figure 1 shows the CIDWM in the Gd-Fe wire. As shown in Fig. 1, the DW in the wire is clearly moved by the electric current. We found that the J_{th} for CIDWM in the Gd-Fe alloy wires is sufficiently small (~3.1×10^{10} A/m^2). This result indicate the amorphous rare-earth transition-metal magnetic alloys is promising material for the magnetic memory.

This work was financially supported by the MEXT-Supported Program for Strategic Research Foundation at Private University (2014-2020), MEXT KAKENHI Grant Number 26630137 (2014-2016), Iketani Science and Technology Foundation, Research Foundation for Electrotechnology of Chubu, and research grant from The Mazda Foundation.

Reference

[1] S. S. P. Parkin, et al., Science **320**, 190 (2008).

[2] D. A. Allwood, et al., Science **309**, 1688 (2005).

No. D5

Spin absorption in a lateral spin valve with ferromagnetic/nonmagnetic bilayer spin channel

T. Ariki[1], D. Itou[1], and T. Kimura[1,2]

[1] *Department of Physics, Kyushu University*

[2] *Research Center for Quantum Nano Spin Sciences,Kyushu University*

Email: t-kimu@phys.kyushu-u.ac.jp

Generation, manipulation and detection of spin currents are important issues for the developments of spintronic devices because a spin current plays an important role in spin-dependent transport and spin-transfer switching. Lateral spin valve structure provides an ideal platform for investigating the intriguing properties of spin current precisely because of its flexible electrode design. Especially, recent development of the highly spin polarized ferromagnetic electrodes enable us to observe the sufficiently large spin-dependent signal even at room temperature. In this talk, I introduce the efficient way for manipulating the spin current by using a lateral spin valve with a nonmagnetic(NM)/ ferromagnetic(FM) metal bilayer spin channel.

As shown in Figs. 1a and 1b, in the NM/FM bilayer channel, since the spin relaxation time depends on the relative angle between the injected spin and the magnetization, the spin accumulation in the NN can be modulated by the magnetization direction. Figure 1c shows the field dependence of the nonlocal spin valve signal. In addition to the conventional signal changes due to the parallel and anti-parallel transitions, the broad signal change is observed during the entire field sweep. This broad change can be quantitatively understood by the modulation of the spin absorption. Since the modulation ratio increases with increasing the spin polarization of the spin absorber, it is possible to produce the spin-resistance switching devices.

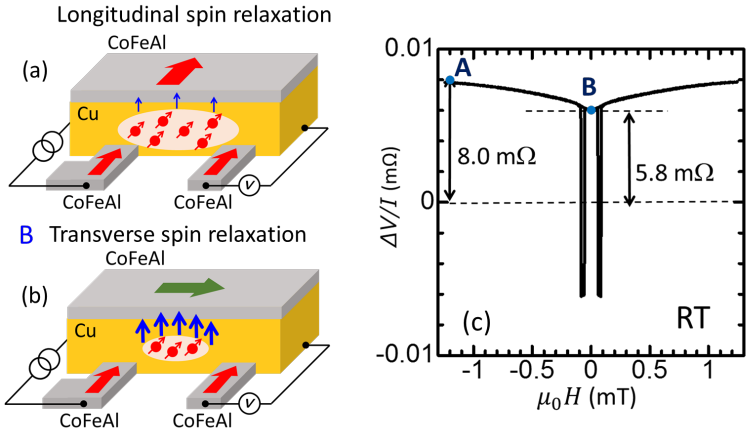

Figure 1. Conceptual image of (a) Longitudinal spin absorption and (b) transverse spin absorption. (c) Observed nonlocal spin valve signal with the spin current modulation.

No. P2

Quantum materials: at the interface between III-nitrides, topological insulators and 2D systems

A. Bonanni[1]

[1] *Johannes Kepler University, Institute for Semiconductor and Solid State Physics, Linz, Austria*

Email: alberta.bonanni@jku.at

We provide a panoramic view of our extensive work on modulated magnetic III-nitride structures [1-14] and we discuss the perspectives for proximity-induced phenomena like topological superconductivity in heterostructures combining epitaxial graded and Rashba III-nitrides with 2D layered *s*-wave superconductors. Moreover, we report on the observation of anomalous Hall effect in thin films of $Sn_{1-x}Mn_xTe$ at T = 8 K for $x \sim 0.07$ [unpublished], as first step towards the unraveling of topologically protected quantum anomalous Hall effect in the SnTe class of topological crystalline insulators. Finally, our recent results on the epitaxial growth of Bi_2Se_3/FeSe bilayers and preliminary *in situ* synchrotron angle-resolved photoemission spectroscopy measurements [unpublished] point at proximity induced topological superconductivity in the 3D topological insulator Bi_2Se_3 and open new perspective for emerging proximity-induced phenomena.

References

[1] A. Bonanni *et al*., Phys. Rev. Lett. **101**, 135502 (2008).
[2] M. Rovezzi *et al.,* Phys. Rev. B **79**, 195209 (2009)
[3] . Navarro-Quezada *et al*., Phys. Rev. B **81**, 205206 (2010)
[4] A. Navarro-Quezada *et al*., Phys. Rev. B **84**, 155321 (2011)
[5] I. A. Kowalik *et al*., Phys. Rev. B **85**, 184411 (2012)
[6] A. Grois *et al*., Nanotechnology **25** 395704 (2014)
[7] A. Bonanni and T. Dietl, Chem. Soc. Rev. **39**, 528 (2010)
[8] T. Dietl *et al*., Rev. Mod. Phys. **87**, 1311 (2015)
[9] T. Devillers *et al*., Scientific Reports **2**, 722 (2012)
[10] T. Devillers *et al*., Appl. Phys. Lett. **103**, 211909 (2013)
[11] G. Capuzzo *et al*., Scientific Reports **7**, 42697 (2017)
[12] R. Adhikari *et al*., Phys. Rev. B **94**, 085205 (2016)
[13] D. Sztenkiel *et al*., Nat. Commun. **7**, 13232 (2016)
[14] A. Navarro-Quezada *et al*., arXiv1809:08894

No. E1

Spin wave spectrum of 3d ferromagnet based on QSGW calculations

H. Okumura[1], K. Sato[1], and T. Kotani[2]

[1] *Graduate School of Engineering, Osaka University, Osaka, Japan*

[2] *Department of Applied Mathematics and Physics, Tottori, Japan*

Email: okumura.haruki@mat.eng.osaka-u.ac.jp

We have developed spin wave (SW) spectrum calculation code, combining quasi-particle self-consistent *GW* (QSGW) and maximum localized Wannier function approach. We adopt the linear response method for the dynamical transverse susceptibility [1], which includes the SW damping by Stoner excitations. Stoner excitation is fundamental in weak ferromagnet (e.g. Fe), while not so important in strong ferromagnet (e.g. Ni) which has the finite Stoner gap.

In both the local density approximation (LDA) and QSGW, we found the SW in Fe is strongly damped by Stoner excitations. On the other hand, the SW in Ni shows more distinguishable peak than Fe. In addition, Fig. 1(a) shows that the LDA overestimates SW energy as deviated from Γ point, which leads to the overestimation of SW stiffness constant *D* (834 meV･Å in average) as compared to experimental value (483 meV･Å). However, Fig. 1(b) shows that the QSGW well reproduce SW energy in the middle of Brillouin zone, especially in [100] direction. Moreover, the D (481 meV･Å) is good agreement with experimental one. In the case of cubic FeCo in ordered state, we found acoustic and optical mode in the SW spectrum.

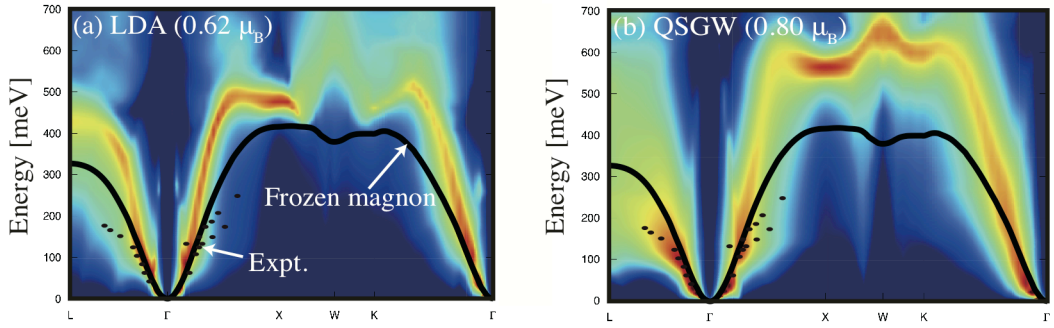

Fig. 1: Spin wave spectrum in Ni with (a) LDA and (b) QSGW. The large intensity of excitations is indicated by warm colors. Solid points are the inelastic neutron scattering experiment [2] and bold line is the frozen magnon calculations [3].

References

[1] C. Friedrich, *et al*., First Principles Approaches to Spectroscopic Properties of Complex Materials (Springer Berlin Heidelberg, Berlin, Heidelberg **347,** 259-301 (2014).

[2] H. A. Mook and D. McK. Paul. *Phys. Rev. Lett.*, **54**, 227 (1985).

[3] M. Pajda, et al., *Phys. Rev*. B, **64**, 174402 (2001).

No. E2

Crystal structure prediction by machine learning

T. Yamashita[1,2]

[1] *National Institute for Materials Science, Tsukuba, Japan*

[2] *Osaka University, Ibaraki, Japan*

Email: yamashita06@cmp.sanken.osaka-u.ac.jp

Predicting the most stable structure for a given chemical composition is a very difficult problem. So far, several approaches to structure prediction for crystalline systems combined with structure optimization methods have been developed such as random search [1] and evolutionary algorithm [2]. We have developed a searching algorithm accelerated by Bayesian optimization [3]. Evolutionary algorithm is one of the structure generation methods, while Bayesian optimization is classified into a selection-type algorithm which can efficiently select potential candidates from a large number of structures using a machine learning technique.

Crystal structure prediction using Bayesian optimization combined with random search is applied to known systems such as NaCl and Y_2Co_{17}. As shown in Fig. 1, the results demonstrate that Bayesian optimization can significantly reduce the number of searching trials required to find the global minimum structure by 30–40% in comparison with pure random search, which leads to much less computational cost.

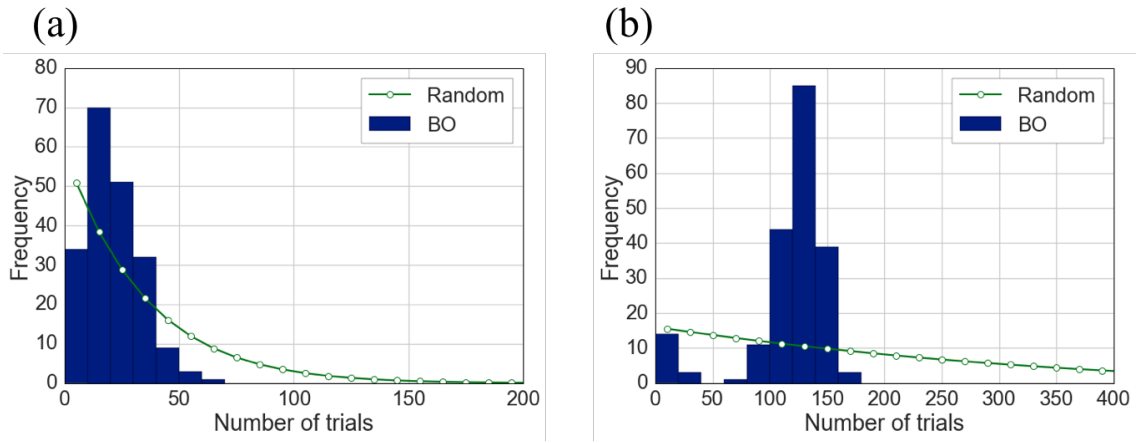

Fig 1. Frequency distribution of number of trials required to find the most stable structure for (a) NaCl and (b) Y_2Co_{17}.

References

[1] C. J. Pickard and R. J. Needs, Phys. Rev. Lett. **97**, 045504 (2006).

[2] A. R. Oganov and C. W. Glass, J. Chem. Phys. **124**, 244704 (2006).

[3] T. Yamashita, N. Sato, H. Kino, T. Miyake, K. Tsuda, and T. Oguchi, Phys. Rev. Materials **2**, 013803 (2018).

No. E3

Property of highly doped magnetic semiconductor - supercell band-structure-calculation approach -

Noriaki Hamada[12], Akira Masago[1], Hikari Shinya[15], Tetsuya Fukushima[134], and Hiroshi Katayama-Yoshida[6]

[1] *Center for Spintronics Research Network, Osaka University, Toyonaka, Japan*
[2] *Faculty of Science and Technology, Tokyo University of Science, Noda, Japan*
[3] *Institute for NanoSciece Design, Osaka University, Toyonaka, Japan*
[4] *Institute for Datability Science, Osaka University, Suita, Japan*
[5] *Graduate School of Engineering, Yokohama National University, Yokohama, Japan*
[6] *Center for Spintronics Research Network, The University of Tokyo, Tokyo, Japan*

So far, we have investigated high Curie temperature spintronics materials, e.g., Fe-doped GaSb and Eu-doped GaN. Fe-doped GaSb compounds are expected as high-speed switching transistors and non-volatile magnetic memories [1]. Eu-doped GaN is renown as a LED, and is expected for a novel spintronics material converting magnetic and optical properties [2].

In this study, we focus 3d-transition-metal-doped GaN and GaSb. The ferromagnetic semiconductor with high Curie temperatures is ingredient essential for the spintronics devices operating at room temperature. As for the host semiconductor, InAs, InSb, and GaSb have been recently attracting much attention [1]. While those semiconductors are characterized by the small bandgap, the most important feature is the lattice constant for interstitial-site doping. For example, in the Ga compound, the lattice parameter in the zincblende structure is listed as

zincblende	GaN	GaP	GaAs	GaSb
lattice const. a [Å]	4.52	5.45	5.65	6.10

The large lattice constant allows us to introduce the 3d atom to the interstitial site.

The band structure calculation was preformed by using the FLAPW method. Our purpose is to see the overall change of the magnetic property on changing the dopant (Ti – Ni).

Magnetic property on changing the dopant is shown here for GaN and GaSb in the zincblende structure.

(1) ZGa_3N_4 (Z = Ti – Cu)

For the GaN-based compound, only the Ga atom is replaced by the 3d-metal atom.

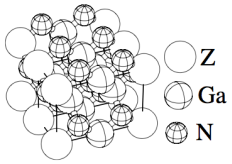

Fig. 1a. Chain-1

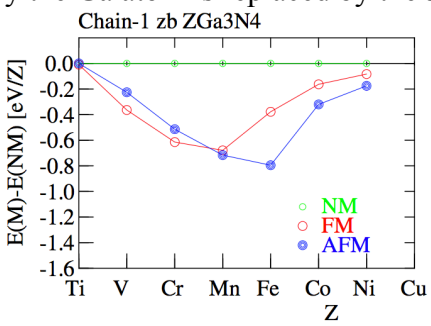

Fig. 1b. Magnetic-ordering Energy

For a 3d-atom chain shown in Fig.1a, the magnetic-ordering energy is plotted in Fig.1b. For Fe, the antiferromagnetic interaction dominates the magnetic property. If we want to obtain a ferromagnetic state, we have to use Cr or V as dopant.

(2) ZGa_3Sb_4 (Z = Ti – Ni) For the GaSb-based compound, the Ga atom is firstly replaced by the 3d-metal atom when the 3d-metal concentration is low.

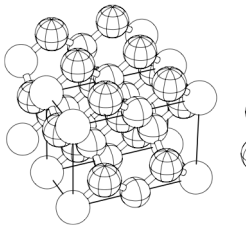

Fig. 2a. Chain-1

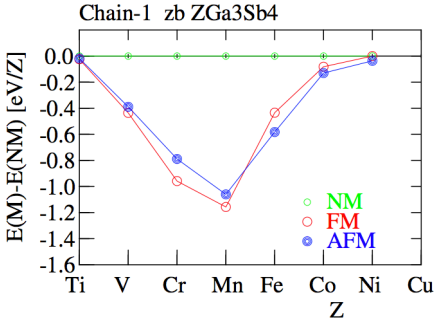

Fig. 2b. Magnetic-ordering Energy

In this case, the magnetic structure is expected to show a similar property to the GaN compound.

(3) $Z_2Ga_3Sb_4$ (Z = Ti – Ni) For higher concentration, the 3d-metal atom occupies the interstitial site. A 1- dimensional chain brings a result as shown in Fig.3. A strong ferromagnetism is expected for Fe.

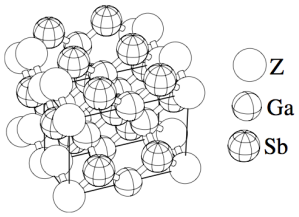

Fig. 3a. Chain-d11

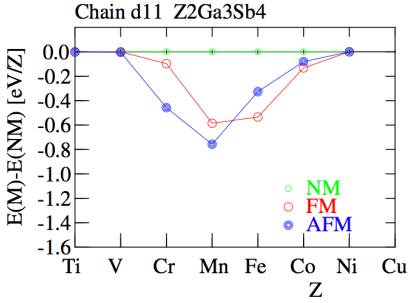

Fig. 3b. Magnetic-ordering Energy

Small bandgap compounds opened a new stage of the strong ferromagnetic semi-conductor. We will elucidate key points to obtain better magnetic semiconductor.

References

[1] Hikari Shinya, Tetsuya Fukushima, Akira Masago, Kazunori Sato, and Hiroshi Katayama-Yoshida, First-principles prediction of the control of magnetic properties in Fe-doped GaSb and InSb, J. Appl. Physics 124, 103902 (2018).

[2] Akira Masago, Tetsuya Fukushima, Kazunori Sato, and Hiroshi Katayama-Yoshida, Computational nano-materials design of self-organized nanostructures by spinodal nano-decomposition in Eu-doped GaN, Jpn. J. Appl. Physics 55, 070302 (2016).

No. E4

Half metallic ferromagnetic quaternary Heusler compounds with high Curie temperatures

B. Sanyal[1], A. Kundu[2], S. Ghosh[2], R. Banerjee[1]and S. Ghosh[2]

[1] *Dept. of Physics and Astronomy, Uppsala University, Uppsala, Sweden*

[2] *Dept. of Physics, Indian Institute of Technology, Guwahati, Assam, India*

Email: Biplab.Sanyal@physics.uu.se

There is a perpetual search for new magnetic materials with high Curie temperatures for spintronic applications. Specifically, materials with half metallic properties are of great interest. Here, we present an ab initio density functional study of the structural, electronic and magnetic properties of quaternary Heusler compounds CoX'Y'Si where X' is a transition metal with 4d electrons and Y' is either Fe or Mn. Five new half-metallic ferromagnets with spin polarisation nearly 100% with very high Curie temperatures have been found. The variation of Curie temperatures as a function of valence electrons can be understood from the calculated inter-atomic exchange interaction parameters. We also identify a few other compounds, which could be potential half-metals with suitable application of pressure or with controlled doping. Our results reveal that the half-metallicity in these compounds is intricately related to the arrangements of the magnetic atoms in the Heusler lattice and hence, the interatomic exchange interactions between the moments. The trends in the atomic arrangements, total and local magnetic moments, interatomic magnetic exchange interactions and Curie temperatures are discussed with fundamental insights.

References

[1] A. Kundu, S. Ghosh, R. Banerjee, S. Ghosh & **B. Sanyal**, Scientific Reports **7**, 1803 (2017).

Abstracts for poster presentations

No. 01

First-principles prediction of the control of magnetic properties in Fe-doped GaSb and InSb

H. Shinya[1,2], T. Fukushima[2,3,4], A. Masago[2], K. Sato[2,5], and H. Katayama-Yoshida[6]
[1]*Graduate School of Engineering, Yokohama National University, Yokohama,*
[2]*Center for Spintronics Research Network, Osaka University, Osaka*
[3]*Institute for NanoScience Design, Osaka University, Osaka*
[4]*Institute for Datability Science, Osaka University, Osaka*
[5]*Graduate School of Engineering, Osaka University, Osaka*
[6]*Center for Spintronics Research Network, The University of Tokyo, Tokyo*
Email: shinya-hikari-sb@ynu.ac.jp

Recently, Fe-doped semiconductors have been attracting much attention as ferromagnetic semiconductors due to the possibility that they may exhibit high Curie temperatures and low power consumption and that they may be useful for high-speed spin devices. High Curie temperature ferromagnetism has been observed in Fe-doped InAs, from which both *n*- and *p*-type ferromagnetic semiconductors can be fabricated. In order to obtain a higher Curie temperature than that of (In,Fe)As, we have focused on GaSb and InSb as host semiconductors. Actually, Curie temperature higher than the room temperature and *n*-type dilute magnetic semiconductors (DMSs) were experimentally observed. For example, the Curie temperature of the Fe 25% doped GaSb is about 350 K. The Fe 16% doped InSb becomes *n*-type DMS and shows the Curie temperature of 330 K. Although the inhomogeneous Fe-rich regions are formed in both systems, the Fe atoms keep the zincblende structure of the host semiconductors without any ferromagnetic secondary precipitation such as FeSb [1,2].

We have investigated the electronic structures, magnetic properties, and structural stability of Fe-doped GaSb and InSb by using the Korringa-Kohn-Rostoker Green's function method within density functional theory. We have found that the isoelectronic Fe-doped GaSb and InSb have strong antiferromagnetic interactions due to the super-exchange mechanism. By considering artificial changes in the Fermi level, we have found that the magnetic exchange coupling constants in these systems exhibit universal behavior. Antiferromagnetic-ferromagnetic transitions occur for both *n*- and *p*-type doping, and this behavior can be well understood in terms of the Alexander-Anderson-Moriya mechanism. The Fermi level dependence of the chemical pair interactions also shows characteristic features, which can be reasonably explained by magnetic frustration and the nature of the covalent bond. Our multi-scale simulations show that finite Curie temperatures are realized in *n*- and *p*-type regions. For *p*-type doping, the spinodal nano-decomposition caused by annealing drastically enhances Curie temperature. However, for *n*-type doping, the initial phases have higher Curie temperatures than the final phases. Based on the results of our calculations, we propose

that high Curie temperatures may be realized and that the magnetic states of (Ga,Fe)Sb and (In,Fe)Sb may be manipulated by controlling the gate voltage, chemical doping, and annealing process. Such features will be very important for next-generation semiconductor spintronics [3].

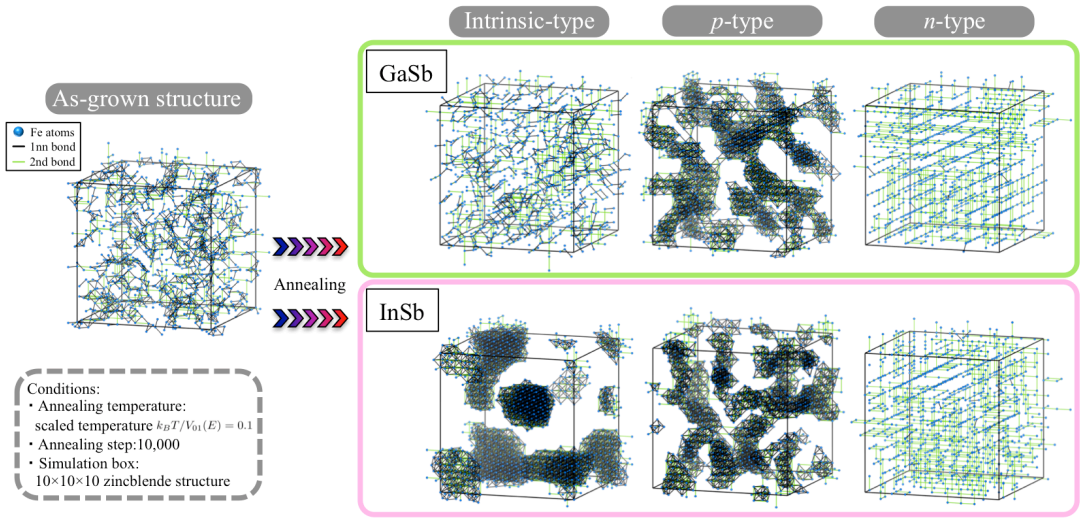

Fig. 1. Snapshots of the Monte Carlo simulation for the spinodal nanodecomposition in (Ga,Fe)Sb and (In,Fe)Sb. Initial phase and annealed phases of intrinsic-, *p*-, and *n*-type (Ga,Fe)Sb and (In,Fe)Sb after 10,000 Monte Carlo steps.

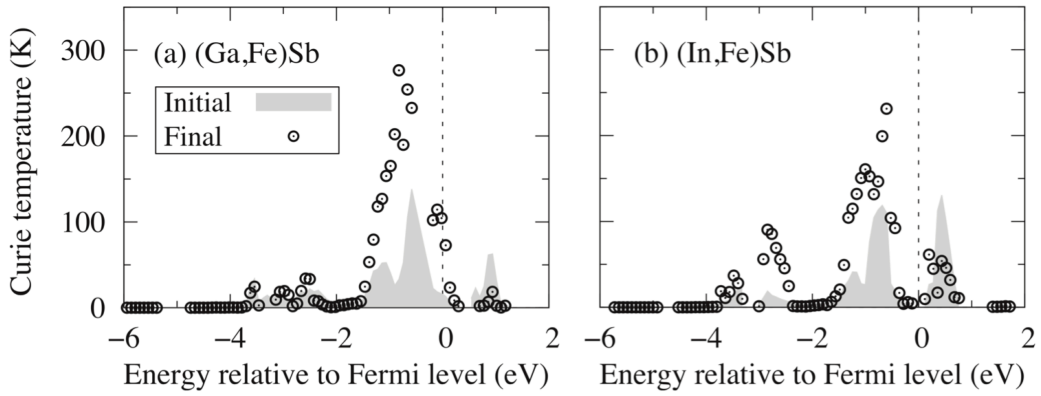

Fig. 2. Curie temperature of (a) (Ga,Fe)Sb and (b) (In,Fe)Sb for the initial (gray areas) and final (points) phases calculated with the random phase approximation as a function of the Fermi level shift. The Fe concentration is fixed at 20%.

References

[1] N. T. Tu, P. N. Hai, L. D. Anh, and M. Tanaka, Appl. Phys. Lett. **108**, 192401 (2016).

[2] N. T. Tu, P. N. Hai, L. D. Anh, and M. Tanaka, Appl. Phys. Express **11**, 063005 (2018).

[3] H. Shinya, T. Fukushima, A. Masago, K. Sato, and H. Katayama-Yoshida, J. Appl. Phys. **124**, 103902 (2018).

No. 02

Size effect on the mechanical behavior of single crystalline Fe-31.2Pd (at%) micropillars

Fei Xiao[1,2] and Takashi Fukuda[2]

[1] *State Key Lab of Metal Matrix Composite, School of Materials Science and Engineering, Shanghai Jiao Tong University, 800 Dong Chuan Road, Shanghai 200240, P. R. China*

[2] *Department of Materials Science and Engineering, Graduate School of Engineering, Osaka University, 2-1, Yamada-oka, Suita, Osaka 565-0871, Japan*

Email: xfei@sjtu.edu.cn

The size effect on the mechanical behaviors of single crystalline Fe-31.2Pd (at%) micropillars with four different pillar diameters (approximately 2 μm, 1 μm, 500 nm and 400 nm) were studied by compressing in the [001] direction. Both the Young's modulus and yield stress increase with the decrease of pillar diameter. The main defects in the plastically deformed pillars are the {111} deformation twins, which could be covered by high density of dislocations after further plastic deformation in a 400 nm pillar. A repeatable elastic-like strain ~4% was observed for more than 40,000 cycles.

No. 03

Design of super-high-T_C high-entropy ferromagnetic semiconductors in Fe-doped III-V compound by spinodal nano-decomposition and volume compensated codoping

H. Shinya[1] T. Fukushima[2], A. Masago[3], K. Sato[4], and H. Katayama-Yoshida[5]

[1] *Graduate School of Engineering, Yokohama National University, Yokohama, Japan*
[2] *Institute for NanoScience and Design, Osaka University, Toyonaka, Osaka, Japan*
[3] *Center for Spintronics Research Network, Graduate School of Engineering Science, Osaka University, Toyonaka, Osaka, Japan*
[4] *Graduate School of Engineering, Osaka University, Suita, Osaka, Japan*
[5] *Center for Spintronics Research Network, Graduate School of Engineering, The University of Tokyo*
Email: hkyoshida@ee.t.u-tokyo.ac.jp

Design and realization of super-high-Curie temperature (T_C) magnetic semiconductors, in which the exchange interactions can be controlled by gating, are essential for the realistic application of semiconductor nano-spintronics.

Recently, Fe-doped III-V-based narrow-gap diluted magnetic semiconductors with high-T_C are successfully grown by MBE, and T_C goes up to above room temperatures [1]. Based on the three general design rules of (1) the volume compensations [VC] by codoping with the substitutional (S) Fe impurity [Fe(S)] and the interstitial (I = tetrahedral (*tetra.*) or octahedral (*octa.*) interstitial site) Fe impurity [Fe(I)] [2], (2) spinodal nano-decomposition [SND] of Fe(S) and Fe(I) caused by the low solubility [3], and (3) high-entropy ferromagnetic semiconductors [HEFS] with reducing the Gibbs's free energy ($F = E - TS$) by increasing the entropy (S) in the disordered and high-concentrations of Fe(S) and Fe(I) with codoping [4], we design the super-high-T_C (T_C > 1000K) HEFS in Fe-doped III-V compound by computational nano-materials design [5]. Fe(S) at the III-element site reduces the volume, while the Fe(I) (I = tetra. or octa. interstitial site) expands the volume in III-V compounds, such as GaAs, GaSb, InAs and InSb, which is called volume compensation. The solubility of Fe(S) and Fe(I) are low due to the positive formation energy, so that the SND occurs due to the positive mixing energy. Based on the codoping of isoelectric Fe(S) and triple donors of Fe(I) with high concentrations more than 15~25% in the thermal non-equilibrium crystal-growth condition, we design the HEFS caused by high-doping concentrations with super-high-T_C based on the strong ferromagnetic double exchange interactions between the Fe(S) and Fe(I) caused by SND.

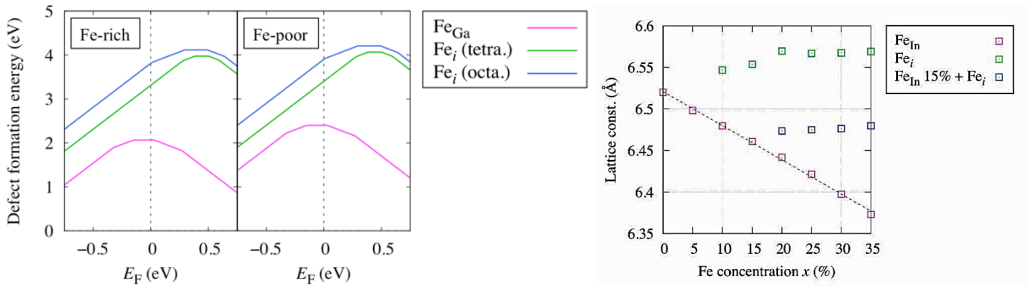

Fig.1: Defect formation energy of Fe at Ga-site (Fe_{Ga}), tetrahedral (Fe_i(tetra.)) and octahedral (Fe_i(octa.)) interstitial sites in GaSb in the Fe-rich and Fe-poor crystal-growth conditions (*see the left two figures*). Lattice constants vs. Fe concentration at the In-site (*lower squares in the right figure*) and at the interstitial site in InSb (*upper squares in the right figure*). After the doping of Fe 15% at the In-sites, then Fe 15% doping at the octahedral interstitial sites, the successive doping indicates V-shape dependence in the lattice constant due to the volume compensations (*see the middle in the right figure*).

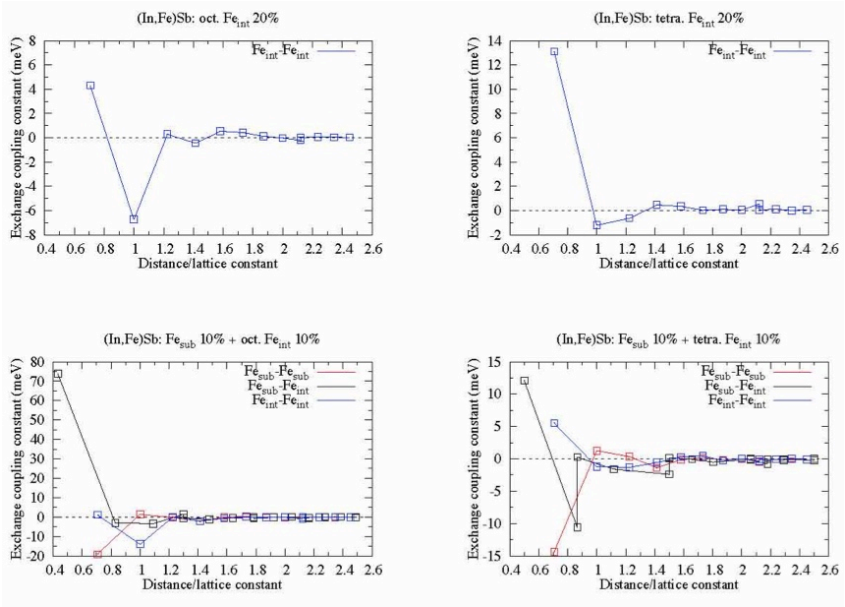

Fig. 2: Exchange interaction vs. distance between Fe impurities at the substitutional (sub.) and interstitial sites (int.) in InSb. It indicates the anti-ferromagnetic super-exchange interaction between the substitutional Fe, on the other hand, the ferromagnetic double exchange interaction becomes dominant between the substitutional and interstitial Fe impurities, and also between the interstitial impurities, where the carriers are caused by the triple donors of interstitial $Fe_{int.}$.

References

[1] P. N. Hai et al. Ohyobutsuri, **87**, 754 (2018).

[2] H. Shinya et al., unpublished data, and J. Appl. Phys. **124**, 103902(2018).

[3] N. D. Vu et al., Jpn. J. Appl. Phys.**53**,110307 (2014).; AIP Conf. Proc. **1583**, 217 (2014).

[4] T. Fukushima et al., Phys. Rev. B**90**, 14417 (2014).

[5] T. Fukushima et al., unpublished data.

No. 04

Fano effect in the transport of an artificial molecule

S. Norimoto S. Nakamura, Y. Okazaki, T. Arakawa, K. Asano,
K. Onomitsu, K. Kobayashi, and N. Kaneko
Graduate School of Science, Osaka University, Osaka, Japan
Email: norimoto@meso.phys.sci.osaka-u.ac.jp

The Fano effect [1] is a ubiquitous phenomenon arising from the interference between a discrete energy state and an energy continuum. It appears in various physical phenomena, for instance, in atomic photoionization, neutron resonance scattering, photoemission, and so on. In mesoscopic systems, too, the Fano effect was demonstrated in a quantum dot embedded in an Aharonov-Bohm ring, where asymmetric Coulomb peaks ("Fano lineshapes") emerge instead of conventional Coulomb peaks with Lorentzian shape [2]. As the Fano effect in nanostructures is attracting many researchers [3], it is of significance to explore electron transport based on this effect in various systems to deepen our understanding of mesoscopic transport.

We experimentally address this effect in an artificial molecule [4], so-called double QDs (DQD), which is two lateral QDs fabricated on conventional GaAs/AlGaAs two-dimensional electron gas system (2DEG) and coupled in series. Conductance measurements for DQD are performed by the standard lock-in technique in a mixing chamber in a dilution refrigerator with a base temperature below 30 mK at zero magnetic field. We found that, when the coupling strength between the leads and QDs is small, the charge stability diagram of the system shows a well-known honeycomb lattice structure that is characteristic of a DQD system. On the other hand, as the coupling increases, a honeycomb structure consisting of the Fano lineshapes is observed to emerge. Our experiment is the first to realize the Fano effect in the artificial molecule.

We assume that the origin of the energy continuum that is necessary for this effect to occur is a strongly-coupled state between the two leads across DQD. Since such a state has large energy width, it eventually works as energy continuum. It coexists with the two discrete energy states in DQD, which have narrower energy width, resulting in the Fano effect. We confirm this scenario by numerical simulation based on the T-matrix method, which can satisfactorily reproduce our observation. Our achievement [4] constitutes a clear example demonstrating the ubiquitous nature of the Fano effect in mesoscopic transport.

References

[1] U. Fano, Phys. Rev. **124**, 1866 (1961).
[2] K. Kobayashi, H. Aikawa, S. Katsumoto, and Y. Iye, Phys. Rev. Lett. **88**, 256806 (2002).

[3] E. Miroshnichenko, S. Flach and Y. S. Kivshar, Rev. Mod. Phys. **82**, 2257 (2010).
[4] S. Norimoto, S. Nakamura, Y. Okazaki, T. Arakawa, K. Asano, K. Onomitsu, K. Kobayashi, and N. Kaneko, Phys. Rev. B **97**, 195313/1-8 (2018).

No. 05

Magnetoresistance and Hall resistance measurements in triangular antiferromagnet Ag_2CrO_2 thin film

Hiroki Taniguchi[1], Shota Suzuki[1], Tomonori Arakawa[1,2], Hiroyuki Yoshida[3], Yasuhiro Niimi[1,2] and Kensuke Kobayashi[1,2]

[1] Graduate School of Science, Osaka University, Japan
[2] Center for Spintronics Research Network, Osaka University
[3] Graduate School of Science, Hokkaido University, Japan
E-mail: taniguchi@meso.phys.sci.osaka-u.ac.jp

Since the discovery of graphene in 2004, there have been many reports on two-dimensional (2D) materials. Especially, 2D materials showing some phase transitions have attracted much attention in terms of the Mermin–Wagner theorem. Recently, two independent groups reported 2D ferromagnetic materials [1,2], which could be useful for future atomic-layer spintronic devices. The motivation of the present study is to find some conductive 2D antiferromagnets and fabricate spintronic devices with them.

Ag_2CrO_2 is one of the layered triangular antiferromagnets with an electrical conductivity [3]. This material shows an antiferromagnetic transition at T_N = 24 K and exhibits a complex magnetic state, the so-called *partially disordered (PD) state*, below T_N [4]. When magnetic moments are arranged on a triangular lattice, it is well-known that the magnetic moments have a large frustration because of the geometrical effect. In this situation, it is theoretically predicted that a unique thermodynamic state, i.e., PD state, appears at finite temperatures [5]. However, the magnetic structure of the PD state is still unclear because the single crystal has not been prepared yet.

In this work, we have developed a new method to obtain higher quality thin films of Ag_2CrO_2 from the polycrystalline samples as shown in Fig. 1, and performed magnetotransport measurements. Figure 2 shows a typical magnetoresistance near the T_N. We observed a clear spin-flip process in the thin film samples, which has never observed in the polycrystalline ones. In the presentation, we will also discuss some results of Hall measurements.

[1] B. Huang *et al*., Nature, **546**, 270 (2017). [2] C. Gong *et al*., Nature, **546**, 265 (2017). [3] H. Yoshida *et al*., J. Phys. Soc. Jpn. **80**, 123703 (2011). [4] Matsuda *et al.,* Phys. Rev. B **85**, 144407 (2012). [5] T. Takagi and M. Mekata, J. Phys. Soc. Jpn. **64**, 4609 (1995). [6] H. Taniguchi *et al*., AIP Adv. **8**, 025010 (2018).

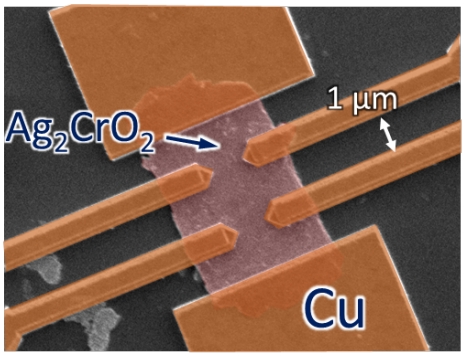

Fig.1 : Scanning electron microscope image of an Ag_2CrO_2 device.

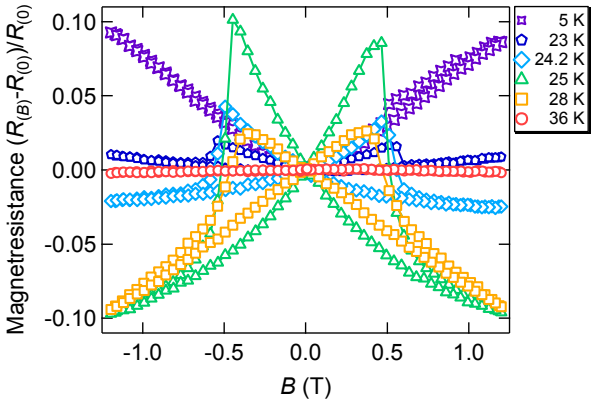

Fig.2 : Magnetoresistance of the Ag_2CrO_2 thin film at different temperatures. The magnetic field is applied perpendicular to the plane.

No. 06

Large anisotropic magnetoresistance induced by a proximity effect in an InAs / (Ga,Fe)Sb quantum well heterostructure

K. Takiguchi[1], L. D. Anh[1,2], K. Okamoto[1], T. Takeda[1], T. Koyama[3], D. Chiba[3] and M. Tanaka[1,4]

[1] *Department of Electrical Engineering and Information Systems, The University of Tokyo,*

[2] *Institute of Engineering Innovation, The University of Tokyo*

[3] *Department of Applied Physics, The University of Tokyo,*

[4] *Center for Spintronics Research Network, The University of Tokyo*

Email: takiguchi@cryst.t.u-tokyo.ac.jp

Fe doped narrow-gap III-V ferromagnetic semiconductor (FMSs), InFeAs, GaFeSb, InFeSb, are promising materials, because Fe atoms are in the neutral state thus do not supply carriers but only local spins in III-V semiconductors, so we can realize both n and p-type and their Curie temperatures can be over room temperature [1,2]. Meanwhile, InAs / GaSb heterostructures have some novel properties; staggered bands, little lattice mismatch (~0.6%), and high electron mobility. In the heterostructure of an InAs quantum well with a GaFeSb barrier, the in-plane transport shows the unique magnetoresistance (MR) originated from the scattering of *s* electrons in InAs as a non-ferromagnet layer with *d* electrons from the magnetization of GaFeSb at the InAs/GaFeSb interface. Note that the resistance of InAs is much lower than that of GaFeSb by more than two orders of magnitude. Therefore, the carriers flow only in the InAs layer. In this study, we observe this MR and modulate it by applying a gate voltage.

We have grown InAs (15 nm) / GaFeSb (15 nm, Fe 20%) / AlSb (300 nm) / AlAs (15 nm) / GaAs (100 nm) on semi-insulating GaAs (001) substrates by low temperature molecular beam epitaxy (Fig. 1(a)). This sample was patterned into a 100 x 200 μm^2 Hall bar; HfO_2 was deposited for a gate insulating layer by atomic layer deposition; the Au gate electrode was fabricated (Fig. 1(b)). In the measurement, we applied the gate voltage from the gate pad to the source electrode and measured the MR by the four terminal method.

Figure 1(c) shows the magnetic field H (= 1 T) angle direction dependence of the resistance when the current J_{DS} = 4.3 μA and the gate voltage V_g = 0 V at 3.5 K. H was rotated (in the *y*-*z* plane) as it was always perpendicular to J_{DS} (// *x* axis), and θ = 0° and 90° means perpendicular to the film plane and in the film plane, respectively. The MR ratio is 2.7%, which is large compared with another study about the in-plane transport of ferromagnet / non-ferromagnet [3][4]. This result means that the electron wavefunction in the InAs penetrates into the GaFeSb even at V_g = 0 V and it is the origin of the anisotropy of the MR. Then, we applied V_g and the MR ratio reaches 7.8% when V_g = −3 V. We can successfully control the electron wavefunction and enhance

the MR in the InAs/GaFeSb heterostructure. In addition, the J_{DS} *vs*. source-drain voltage V_{DS} shows the transistor behavior, which means J_{DS} is greatly modulated by V_g, and

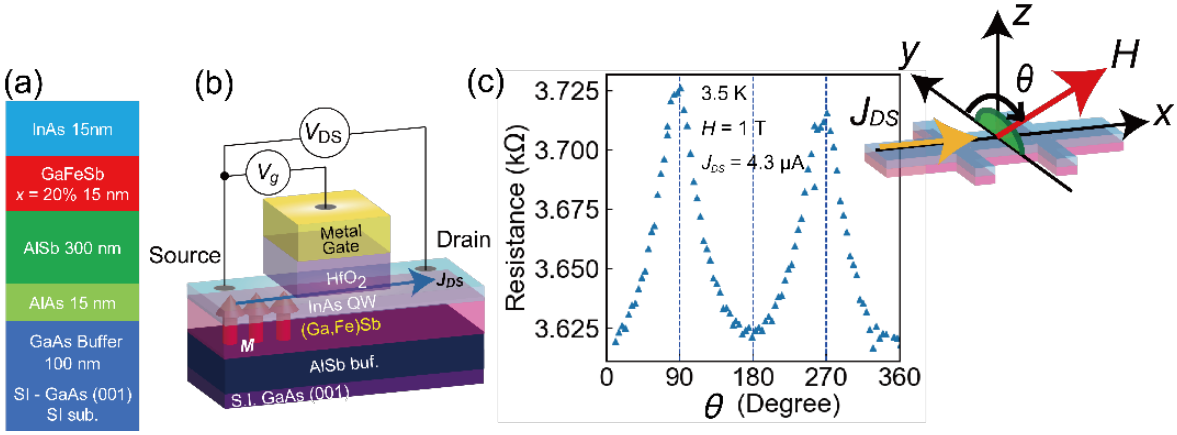

Figure 1 Schematic (a) sample. and (b) device structure with the gate electrode.
(c) Magnetic field direction dependence of the resistance when V_g = 0 V.

finally we confirmed that this device behaves like a magnetic transistor.

This work was supported by Grants-in-Aid for Scientific Research (Grant No. 16H02095, 15H03988,17H0492), CREST of JST, the Yazaki Foundation, and the Murata Science Foundation. Part of this work was carried out under the Spintronics Research Network of Japan.

References

[1] P. N. Hai, *et al.,* Appl. Phys. Lett. **101**, 182403 (2012).
[2] N. T. Tu, *et al.,* Appl. Phys. Lett. **108**, 192401 (2016); arXiv 1706.00735.
[3] H. Nakayama, *et al.,* Phys. Rev. Lett. **110**, 206601 (2013).
[4] C. O. Avci, *et al.,* Nat. Phys. **11**, 570 (2015).

No. 07

Spatial distribution of substitutional Mn-As clusters in ferromagnetic (Zn,Sn,Mn)As_2 thin films revealed by image reconstruction of atom probe tomography

H. Oomae[1], H. Shinoda[1], J. T. Asubar[2], K. Sato[1], H. Toyota[1], K. Mayama[3], B. Medhiyev[4], and N. Uchitomi[1]

[1] *Nagaoka University of Technology, Nagaoka, 940-2188, Japan*

[2] *University of Fukui, Fukui 910-8507, Japan*

[3] *Toshiba Nanoanalysis Corporation, Yokohama 235-8522, Japan*

[4] *National Academy of Sciences of Azerbaijan, AZ 1143, Baku Azerbaijan*

Email: uchitomi@nagaokaut.ac.jp

Ferromagnetic transition in (Zn,Sn,Mn)As_2 thin films is explained by magnetic percolation with Mn-As clustering network [1]. We studied the spatial relationship of Mn-As clusters with the resulting Curie temperature (T_C) in the materials, assuming the reconstruction of local atomic structures from dataset of atomic positions in (Zn,Sn,Mn)As_2 obtained by atom probe tomography (APT). To probe local atomic structures and magnetic properties of Mn-As cluster in $ZnSnAs_2$ thin films, we investigated (Zn,Sn,Mn)As_2 samples doped with 2.1 and 3.6 at. % Mn, which were grown on (001) InP substrates by molecular beam epitaxy. Several representative regions with low and high Mn concentration were extracted from APT dataset. Mn-As clusters consisting of 2 - 36 Mn-As cluster configurations in the reconstructed local structures of high Mn concentration regions were identified. We also obtained a correlation between T_C and Mn-As clustering consistent not only with the experimental results but also with the first principles calculation using mean-field approximation.

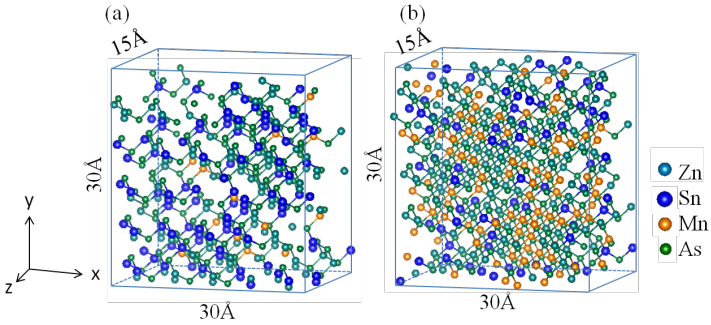

Reconstruction lattice of (a) low Mn concentration region and (b) high Mn concentration region. The atomic positions are determined on the assumption of a sphalerite structure with lattice parameters of a = 5.85, b = 5.85, and c = 11.7 Å.

Reference

[1] N. Uchitomi,S. Hidaka, et al., J. Appl. Phys. **123**, 161566 (2018)

No. 08

A first-principles study on the magnetism of Fe/Bi/MgO multilayers

K. Hiraoka and T. Oguchi
Institute of Scientific and Industrial Research, Osaka University
Email: hiraoka@cmp.sanken.osaka-u.ac.jp

The magnetic tunnel junction (MTJ) has a structure consisting of two ferromagnetic layers separated by a thin insulating layer. MTJ is used for the magnetoresistive random access memory (MRAM) cell with giant magneto resistance ratio. MRAM is a nonvolatile memory without requiring standby power to keep information and has attracted much attention as a new generation of low power consumption memory. Strong perpendicular magnetic anisotropy to realize high density memory devices is highly desired for preventing thermal magnetic fluctuation in the ferromagnetic layer of MTJ. Perpendicular magnetic anisotropy originates from magnetocrystalline anisotropy (MCA) caused by spin-orbit coupling. In this study, we investigate the influence of a Bi layer insertion at Fe/MgO interface by first-principles density-functional calculations. We first propose models of Fe/Bi/MgO by considering lattice matching for the calculations and then study the magnetism of Fe/Bi/MgO as well as Fe monolayer and Fe/MgO films. It is found that enhancement in perpendicular magnetic anisotropy can be obtained by inserting the Bi layer at the Fe/MgO interface. The electronic origin of MCA in the systems is discussed from the viewpoint of Bruno's formula [1] and band structure within the second-order perturbation theory [2].

References

[1] P. Bruno, Phys. Rev. B **39**, 865 (1989).
[2] D. S. Wang, R. Wu, and A. J. Freeman, Phys. Rev. B **47**, 14 932 (1993).

No. 09

Growth of Fe_4N films toward fabrication of Fe_4N-based current-perpendicular-to-plane giant magnetoresistance devices

K. Ito[1,2], T. Kubota[1,2], and K. Takanashi[1,2]

[1] *Institute for Materials Research, Tohoku University, Sendai, Japan*

[2] *Center for Spintronics Research Network, Tohoku University, Sendai, Japan*

Email: itok@imr.tohoku.ac.jp

Anti-perovskite type 3*d* transition metal ferromagnetic nitrides are a promising candidate as a new spintronics material. Fe_4N, one of these compounds, is theoretically predicted to have a large negative spin-polarization of electrical conductivity ($P_\infty = -1.0$) [1]. In addition, large tunnel magnetoresistance effect is theoretically expected due to coherent tunneling in the Fe_4N/MgO/Fe_4N magnetic tunnel junction with perpendicular magnetic anisotropy [2], and voltage control of magnetocrystalline anisotropy in Fe_4N/MgO is predicted by theoretical calculations [3]. On the other hand, we consider that the large $|P_\infty|$ and relatively high electrical resistivity of Fe_4N is suitable for application to a current-perpendicular-to-plane giant magnetoresistance (CPP-GMR) recording head of a next generation hard disk drive [4]. In this work, we grew Fe_4N epitaxial films by molecular beam epitaxy toward fabrication of Fe_4N-based CPP-GMR devices.

The Fe_4N film was grown on $SrTiO_3$(STO)(001) substrates at 500 °C by supplying Fe and radio-frequency N_2 plasma, simultaneously. Figures 1 and 2 show the reflection high-energy electron diffraction (RHEED) and out-of-plane x-ray diffraction (XRD) patterns of the Fe_4N film, respectively. Epitaxial growth of the Fe_4N film on the STO(001) substrate was confirmed. As a next step, we try to grow Fe_4N films on a metallic buffer layer, and Fe_4N/non-magnetic metal/Fe_4N tri-layer structure.

References

[1] S. Kokado *et al*., Phys. Rev. B **73**, 172410 (2006). [2] B. Yang *et al*., Phys. Rev. Appl. **9**, 1054019 (2018). [3] Z. R. Li *et al*., Appl. Phys. Lett. **113**, 132401 (2018). [4] M. Takagishi *et al*., IEEE Trans. Magn. **46**, 2086 (2010).

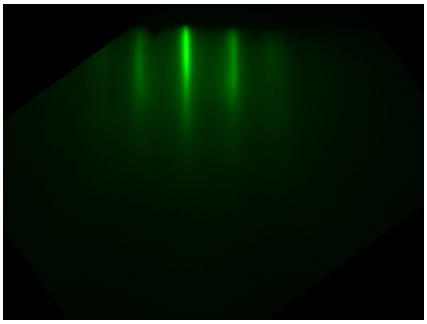

Fig. 1 RHEED pattern of the Fe_4N layer.

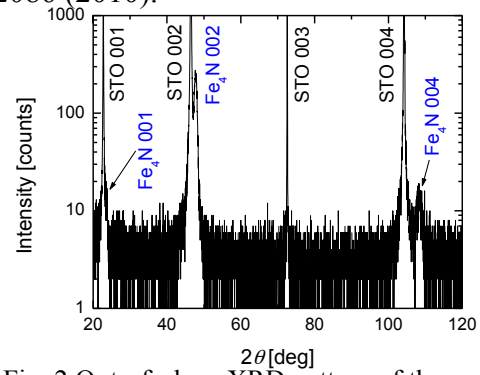

Fig. 2 Out-of-plane XRD pattern of the sample.

No. 10

First-principles study on anomalous Hall conductivity in anti-perovskite manganese nitrides Mn_3MN (M= Ni, Cu, Ga, Ge, In, Sn, Ir) with antiferromagnetic structures

Vu Thi Ngoc Huyen[1,2,3], Michi-To Suzuki[4], Kunihiko Yamauchi[2] and Tamio Oguchi[2]

[1] *Graduate School of Engineering Science, Osaka University, Osaka 560-853, Japan*
[2] *Institute of Scientific and Industrial Research, Osaka University, Osaka, Japan*
[3] *National Institute for Materials Science, Osaka, Japan*
[4] *Institute for Materials Research, Tohoku University, Sendai, Japan*
Email: vnhuyen@cmp.sanken.osaka-u.ac.jp

Anomalous Hall (AH) effect was known being able to appear with certain magnetic symmetry in the absence of external magnetic fields [1]. Therefore, this effect can be used for probing spin polarization of electrons in nanoscale systems and memory devices [2]. Conventionally, the AH effect was assumed to be proportional to magnetization leading to no AH conductivity in antiferromagnets with no net magnetization. Nevertheless, the first-principles calculation has predicted the large AH conductivity for the non-collinear antiferromagnet with no net magnetization in Mn_3Ir [3]. Following the finding, non-collinear antiferromagnet Mn_3Ge and Mn_3Sn have been studied to explain the AH effect theoretically and experimentally [2,4–8]. This attractive content of non-collinear antiferromagnetism urges us to search for new materials for spintronic applications. A neutron diffraction experiment reported that some anti-perovskite manganese nitrides Mn_3MN show antiferromagnetism with a triangular magnetic ordering [9]. So Mn_3MN may be candidates for antiferromagnetic spintronic applications. In the present work, we study the structural stability of anti-perovskite manganese nitrides Mn_3MN (M= Ni, Cu, Ga, Ge, In, Sn, Ir) by first-principles calculations. Most of the anti-perovskite manganese nitrides are stable in two non-collinear antiferromagnetic configurations, one kind of which can induce AH effect. The AH conductivity is evaluated by using the Wannier interpolation scheme. In order to understand the microscopic mechanism of the AH conductivity in a non-collinear magnetic system, we discuss the cases of large and small AH conductivity by the cluster multipole theory and electronic band structure analysis. The contribution of the Berry curvature to the AH conductivity is also investigated.

References

[1] S. Naoto Nagaosa, Jairo Sinova, Shigeki Onoda, A. H. Mac- Donald, and N. P. Ong, Rev. Mod. Phys. **82**, 1539 (2010).
[2] S. Nakatsuji, N. Kiyohara1, and T. Higo, Nature **527**, 212 (2015).

[3] H. Chen, Q. Niu, and A. H. MacDonald, Phys. Rev. Lett. **112**, 017205 (2014).
[4] J. Kübler and C. Felser, Europhys. Lett. **108**, 67001 (2014).
[5] N. Kiyohara, T. Tomita, and S. Nakatsuji, Phys. Rev. Applied **5**, 064009 (2016).
[6] A. K. Nayak, J. E. Fischer, Y. Sun, B. Yan, J. Karel, A. C. Komarek, C. Shekhar, N. Kumar, W. Schnelle, J. Kübler, C. Felser, and S. S. P. Parkin, Sci. Adv. **2**, e1501870 (2016).
[7] H. Yang, Y. Sun, Y. Zhang, W.-J. Shi, S. S. P. Parkin, and B. Yan, New J, Phys. **19** 015008 (2017).
[8] M.-T. Suzuki, T. Koretsune, M. Ochi, and R. Arita, Phys. Rev. B **95**, 094406 (2017).
[9] D. Fruchart and E. F. Bertaut, J. Phys. Soc. Jpn. **44**, 3(1978).

No. 11

Observation of impurity band related transitions in high Curie temperature *p*-type ferromagnetic semiconductor (Ga,Fe)Sb

Karumuri Sriharsha[1], Le Duc Anh[1,2], Nguyen Thanh Tu[1] and Masaaki Tanaka[1,3]

[1]*Department of Electrical Engineering and Information Systems, The University of Tokyo*

[2]*Institute of Engineering Innovation, The University of Tokyo*

[3]*Center for Spintronics Research Network (CSRN), The University of Tokyo*

Email: harsha@cryst.t.u-tokyo.ac.jp

Recently, new Fe doped narrow-gap ferromagnetic semiconductors (FMSs) such as p-type (Ga,Fe)Sb [1] and n-type (In,Fe)Sb [2] have shown high-Curie temperature (T_C) ferromagnetism, which is essential for the realization of semiconductor spintronic devices operating at room temperature. Understanding the band structure, especially the position of the Fermi level (E_F), of these materials is strongly required to elucidate the origin of high-T_C ferromagnetism as well as their device applications. In this study, using magnetic circular dichroism (MCD) spectroscopy in an infrared region (photon energy E_{ph} = 0.6 – 1.7 eV), we study the band structure of a series of $(Ga_{1-x},Fe_x)Sb$ samples with various Fe densities x = 2, 6, 10 and 20%. We report evidence for the presence of an impurity band (IB) in the band gap of (Ga,Fe)Sb with the E_F lying inside IB.

The samples examined in this work consist of, from the surface, $(Ga_{1-x},Fe_x)Sb$ (15 nm)/AlSb (300 nm)/AlAs (10nm)/GaAs (50nm), grown on semi-insulating GaAs (001) substrates by molecular beam epitaxy. The transport and magnetic properties of these samples were characterized by Hall measurements and MCD with visible – ultraviolet light (E_{ph} = 1.4 – 6 eV). Samples with x = 6, 10 and 20% show ferromagnetism with T_C = 15, 75 and >320 K, respectively. The MCD spectra in infrared region (E_{ph} = 0.6 - 1.5 eV) of these (Ga,Fe)Sb samples and a reference sample of GaSb thin film, measured at 9 K and 1 T, are shown in Fig. 1. The MCD spectra of the (Ga,Fe)Sb samples show two large peaks, a positive peak E_a lying close to the E_0 transition of GaSb (~0.8 eV) and a new negative peak E_b (~1.4 eV). When x is increased from 2 to 20%, the positions of these two peaks linearly move in opposite directions; E_a shifts to lower energy (from 0.84 eV to 0.54 eV) while E_b shifts to higher energy (from 1.41 eV to 1.58 eV) as shown in Fig 2. The values at x > 6% are smaller than the intrinsic band gap of GaSb (~0.8 eV) indicating the presence of IB in the band gap of $(Ga_{1-x},Fe_x)Sb$ with the E_F lying inside it. As illustrated in Fig 3, E_a likely corresponds to the transition at the Γ point from E_F (in the IB) to the conduction band bottom (Γ_6), while E_b corresponds to the transition at the L point from the valence band (VB) (L_6) to E_F. With increasing x, the IB, which is located close to the VB top at small x, broadens and extends towards the band gap, thereby raising the E_F above the VB top, resulting in the red shift in E_a and the blue shift in E_b. The information of the IB and the position of E_F in (Ga,Fe)Sb revealed in this work is crucial for understanding the magnetic properties and spin device applications of this promising high-T_C FMS.

This work was partly supported by Grants-in-Aid for Scientific Research (No. 17H04922), CREST of JST (No. JPMJCR1777), Yazaki Foundation, and the Spintronics Research Network of Japan (Spin-RNJ).

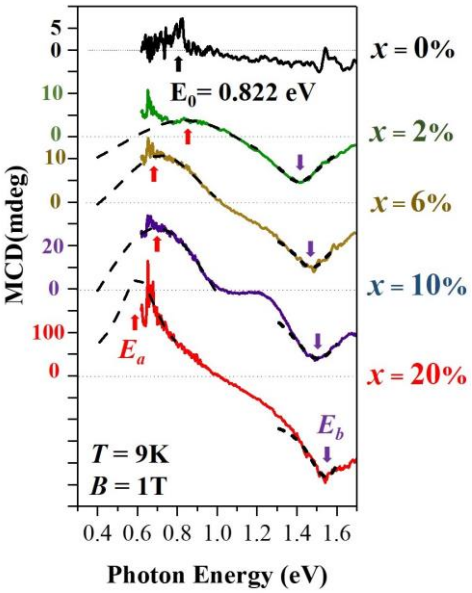

Fig 1. Infrared MCD spectra for the $(Ga_{1-x},Fe_x)Sb$ samples with different Fe densities x (= 0 – 20%).

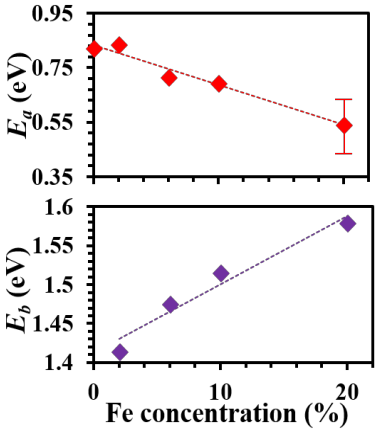

Fig 2. Positions of the E_a and E_b peaks with different Fe density x (= 0 – 20%). For the x = 20% sample, the peak is outside the detectable range, causing the uncertainty.

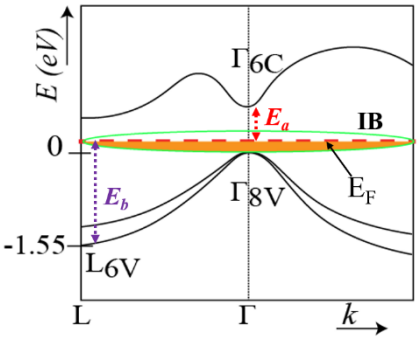

Fig 3. Band structure of (Ga,Fe)Sb showing an impurity band in the band gap and the transitions corresponding to E_a and E_b.

References
[1] N. T. Tu, *et al.*, PRB **92**, 144403 (2015).
[2] N. T. Tu, *et al.*, *APEX* **11** 063005 (2018).

No. 12

Evaluation of temperature-dependent spin Hall angle in CoFeB/MgO/Pt tunneling junctions by using Spin Hall effect tunneling spectroscopy

K. Nakagawara[1], S. Kasai[2], S. Mitani[2], S. Karube[1], M. Kohda[1,3], and J. Nitta[1,3]

[1]*Department of Materials Science, Graduate School of Engineering, Tohoku University, Sendai, Japan*

[2] *National Institute for Materials Science, Tsukuba, Japan*

[3]*Center for Spintronics Research Network, Tohoku University, Sendai, Japan*

Email: knaka@dc.tohoku.ac.jp

Spin Hall effect (SHE) and its inverse effect (i-SHE) are promising ways to generate and to detect spin currents, respectively. The spin Hall angle θ_{SH} is a measure of the conversion efficiency between charge current and spin current. Various methods to evaluate θ_{SH} have been demonstrated [1]-[3]. Recently, SHE tunneling spectroscopy (SHT) [4] has been proposed as an alternative way to evaluate θ_{SH}. In this method, i-SHE signal is obtained via tunneling spin-polarized currents. By using lateral spin valves, spin Hall mechanism (intrinsic and extrinsic spin Hall effect) of Pt has been investigated[5]. In addition to this, the mechanism is also investigated in harmonic measurements[6].

In this study, we experimentally demonstrated the detailed spin-dependent transport mechanism in the spin Hall effect tunneling devices for further understanding the mechanism of spin Hall effect. This method has the potential to measure the temperature-dependent-density of state for evaluation of intrinsic mechanism directly.

Film stack of Ru (8)/Ta (5)/CoFeB (4)/MgO (2)/Pt (7) (thickness in nm) was prepared by magnetron sputtering. The SHT device as shown in Fig.1. One is fabricated by using electron beam lithography and Ar ion milling. CoFeB/MgO junction is patterned into the 4×4 μm^2 square-shaped element. The magneto-transport is measured by using the AC resistance bridge at each temperature. Figure 2 and 3 show an obtained SHT signal, and temperature-dependent spin Hall angle, respectively. The conductivity of this sample is corresponding to the extrinsic mechanism dominant region, but the value is slightly high compared to the spin valve measurement. The further discussion of spin Hall mechanism is undergone.

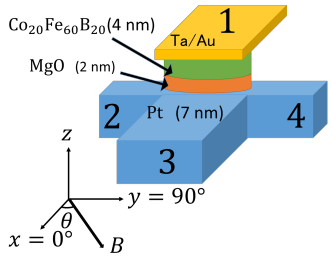

Fig. 1: Sample configuration of SHT device

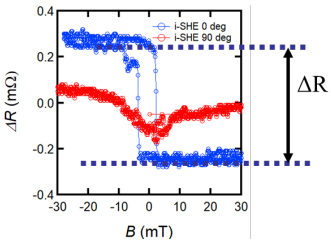

Fig. 2: angular-dependent SHT signal

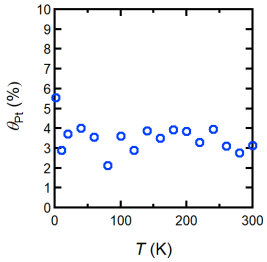

Fig. 3: Temperature-dependent spin Hall angle

References

[1] E. Saitoh *et al.*, Appl. Phys. Lett. **88**, 182509 (2006).
[2] L. Liu *et al.*, Science **336**, 555 (2012).
[3] V. Laurent, *et al.*, Phys. Rev. Lett. **99**, 226604 (2007).
[4] L. Liu *et al.*, Nature Phys. **10**, 561 (2014).
[5] E. Sagasta *et al.*, Phys. Rev. B **94**, 060412 (2016).
[6] G. V. Karnad *et al.*, Phys. Rev. B **97**, 100405 (2018).

No. 13

Study on the magnetization dynamics in magnetic thin films using our proposed measurement technique

Y. Endo[1,2,3], O. Mori[4], Y. Shimada[1,4], S. Yabukami[5], S. Sato[4], and R. Utsumi[4]

[1] *Graduate School of Engineering, Tohoku University, Sendai, Japan*

[2] *Center for Spintronics Research Network (CSRN), Tohoku University, Sendai, Japan*

[3] *Center for Science and Innovation in Spintronics (CSIS), Organization for Advanced Studies, Tohoku University, Sendai, Japan*

[4] *Toei Scientific Industrial Co., Itd., Natori, Japan*

[5] *Graduate School of Biomedical Engineering, Tohoku University, Sendai, Japan*

Email: endo@ecei.tohoku.ac.jp

The magnetization dynamics in magnetic thin films have been studied intensively from both scientific and application points of view. The dynamics are described using phenomelogical Landau-Lifshitz-Gilbert (LLG) equation consisting of both the precession torque of the magnetization and the damping torque [1]. In particular, a Gilbert damping constant (α), which describes the strength of damping torque, is one of the most important parameters to understand the magnetization dynamics. Until now, we proposed a new measurement technique which enables simultaneous evaluation of α and satureation magentostriction (λ_s) by measuring the correlation between ferromagnetic resonance (FMR) frequency (f_r) and the tensile stress, and clarified a correlation between α and λ_s for 50-nm thick Ni-Fe films[2]. Herein, the magnetization dynamics of 10-nm thick Ni-Fe films was investigated by our proposed measurement technique, and the correlation between α and λ_s in these films was discussed.

Figure 1 shows FMR spectra of 10-nm-thick Ni_xFe_{100-x} films either with tensile stress or with tensile stress free. In case of x=78.2 (Fig. 1(a)), each value of FMR frequency with tensile stress ($f_{r\sigma}$) is higher than that of FMR frequency with tensile stress free (f_{r0}) because of uniaxial magnetostrictive anisotropy. The frequency difference ($\Delta f_r = f_{r\sigma} - f_{r0}$) in the external magnetic field (H_{ex}) decreases from +350 to +100 MHz as H_{ex} increases. λ_s evaluated using the $f_{r\sigma}$, f_{r0}, and Δf_r is approximately +1.58 ppm, and is in good agreement with that measured by the optical cantilever method (+3.64 ppm). α is evaluated from f_{r0} and the half-width of the FMR peak with tensile stress free, and is approximately 0.00626. On the other hand, in case of x=84.0 (Fig. 1(b)) every value of $f_{r\sigma}$ is lower than that of f_{r0}. Δf_r in H_{ex} increases from –428 to –34 MHz as H_{ex} increases. λ_s evaluated using the $f_{r\sigma}$, f_{r0}, and Δf_r is approximately –1.25 ppm and agrees well with that measured by the optical cantilever method (–2.91 ppm). α is approximately 0.0107. Furthermore, to clarify the correlation between α and λ_s for 10-nm thick Ni-Fe films, α is plotted in Fig. 2 as a function of λ_s. In the range of positive saturation magnetostriction (λ_s>0), α slightly increases as x decreases, but α increases from 0.00947 to 0.0178 as x increases for negative saturation magnetostriction

(λ_s<0). α reaches a minimum when λ_s is around zero at x = 0.78. This result suggests that the different increment of α depends on positive or negative λ_s. Thus, α and λ_s show a more consistent relation, suggesting that they both originate from spin-orbital coupling [3]. Therefore, these results suggest a correlation between the magnetoelastic properties and α in the Ni_xFe_{100-x} thin films.

This work was supported in part by JSPS KAKENHI Grant Number JP17H03226. This work was also supported in part by CIES collaborative research from CIES, Tohoku University and Advanced Storage Research Consortium (ASRC) in Japan.

References

[1] T. L. Gilbert, IEEE Trans. Magn. **40**, 3443 (2004).
[2] Y. Endo, O. Mori, Y. Shimada, S. Yabukami, S. Sato, and R. Utsumi, Appl. Phys. Lett. **112**, 252403 (2018).
[3] V. Kamberský, Can. J. Phys. **48**, 2906 (1970).

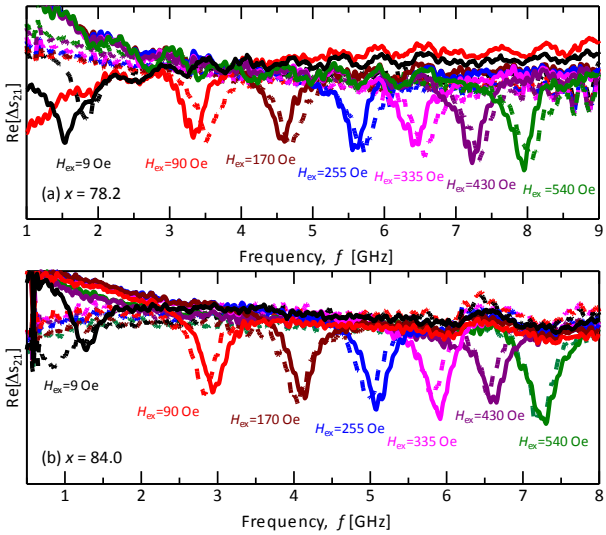

Fig. 1

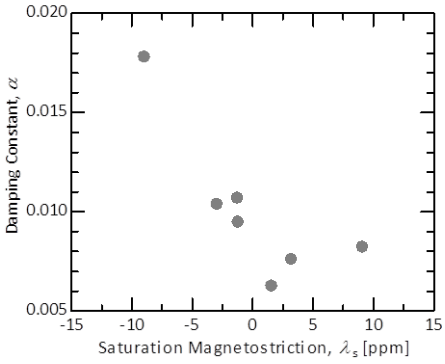

Fig.2

Fig. 1. FMR spectra in various external magnetic fields (H_{ex}) of 10-nm thick Ni_xFe_{100-x} films ((a) x=78.2 and (d) x=84.0) either with tensile stress or with tensile stress free. The dotted line and solid line represent FMR spectra with tensile stress and with tensile stress free, respectively.

Fig. 2. Relationship between the damping constant (α) and the saturation magnetostriction (λ_s) in 10-nm thick Ni_xFe_{100-x} films.

No. 14

Observation of peculiar magnetic anisotropy at the interface of a $La_{0.6}Sr_{0.4}MnO_3/LaAlO_3$ heterostructure

°Le Duc Anh[1,2], Noboru Okamoto[1], Munetoshi Seki[1,3], Hiroshi Tabata[1,3], Masaaki Tanaka[1,3], Shinobu Ohya[1,2,3]

[1]*Department of Electrical Engineering and Information Systems, The University of Tokyo*

[2]*Institute of Engineering Innovation, Graduate School of Engineering, The University of Tokyo*

[3]*Center for Spintronics Research Network, Graduate School of Engineering, The University of Tokyo*

Email: anh@cryst.t.u-tokyo.ac.jp

Control of magnetic anisotropy (MA) is crucial for low-power magnetization reversal in magnetic thin films, which is important for next generation quantum spintronics device applications. From the perspectives of energy efficiency and scalability, gate-voltage control of the MA via modulation of the carrier density and thus, the Fermi level, is highly desirable. For efficient control of MA and for developing materials that are suitable for the MA control, it is necessary to understand the MA of magnetic thin films over a wide energy range; however, there are few studies from this point of view. In ferromagnetic (FM) materials, the MA energy is related to the magnetization-direction dependence of the density of states (DOS) via the spin orbit interaction. Tunneling anisotropic magnetoresistance (TAMR) is a phenomenon observed in tunnel diodes composed of ferromagnetic (FM) layer/ tunnel barrier/ nonmagnetic (NM) electrode. TAMR is defined as the change of the tunnel resistance or conductance dI/dV, which is proportional to the DOS of the electrodes, when rotating the magnetization of the FM layer. Thus, TAMR is useful to understand the magnetic-field direction dependence of the DOS. By measuring TAMR at various bias voltages, one can obtain a high-resolution carrier-energy-resolved map of MA of the FM layer [1].

In this study, using TAMR, we investigate the energy dependence of the MA of the perovskite oxide $La_{0.6}Sr_{0.4}MnO_3$ (LSMO) [2], which is a promising spintronic material due to its half-metallic band structure [3], high Curie temperature (~ 370 K), and colossal magnetoresistance [4]. At the LSMO interface, reconstruction of orbital, charge, and spin configurations occurs due to local structure modifications such as lattice strain and oxygen octahedral rotation, which are only detectable by highly surface-sensitive probes. Understanding these interfacial magnetic properties of LSMO will enable the engineering of the material at an atomic scale, and is thus highly demanded.

The tunnel device structure studied here consists of LSMO (40 unit cell (uc))/ $LaAlO_3$ (LAO, 4 uc) grown on a Nb-doped (0.5 wt%) $SrTiO_3$ (001) (Nb:STO) substrate by molecular beam epitaxy [Fig. 1(a)]. Two-terminal measurements were carried out for 600×700 μm^2 mesa diodes, and the bias polarity was defined so that electrons flow from Nb:STO to LSMO in the positive bias [Fig. 1(b)]. Figure 1(c) shows the change in the tunneling conductance dI/dV with the bias voltage V ranging from –0.5 to +0.5 V applying a magnetic field of 1 T at an angle Φ from the [100] axis in the plane. In addition to the biaxial MA along <100> and the uniaxial MA along [100], which originate from bulk LSMO, we found a peculiar uniaxial MA along the [110], which is attributed to the LSMO/LAO interface. The symmetry axis of this interface MA rotates by 90° at an energy of 0.2 eV below E_F of LSMO, which is attributed to the transition from the e_g band (>–0.2 eV) to the t_{2g} band (<–0.2 eV). These findings hint an efficient way to control the magnetization at the LSMO thin film interfaces, as well as confirm the rich of hidden properties at thin film interfaces that can be revealed only by interface-sensitive probes. This work indicates that the TAMR measurement is a simple but highly sensitive method for characterizing interfacial magnetic properties of MTJs, which is important for developing spintronics devices [5].

This work was supported by Grants-in-Aid for Scientific Research, CREST of JST, and Spin-RNJ.

References:
[1] I. Muneta, T. Kanaki, S. Ohya, and M. Tanaka, Nature Commun. **8**, 15387 (2017).
[2] T. Matou, K. Takeshima, L. D. Anh, M. Seki, H. Tabata, M. Tanaka, and S. Ohya, Appl. Phys. Lett. **110**, 212406 (2017).
[3] J. Park *et al.*, Nature **392**, 794-796 (1998).
[4] A. Urushibara *et al.*, Phys. Rev. B **51**, 14103 (1995).
[5] L. D. Anh, N. Okamoto, M. Seki, H. Tabata, M. Tanaka, and S. Ohya, Sci. Rep. **7**, 8715 (2017).

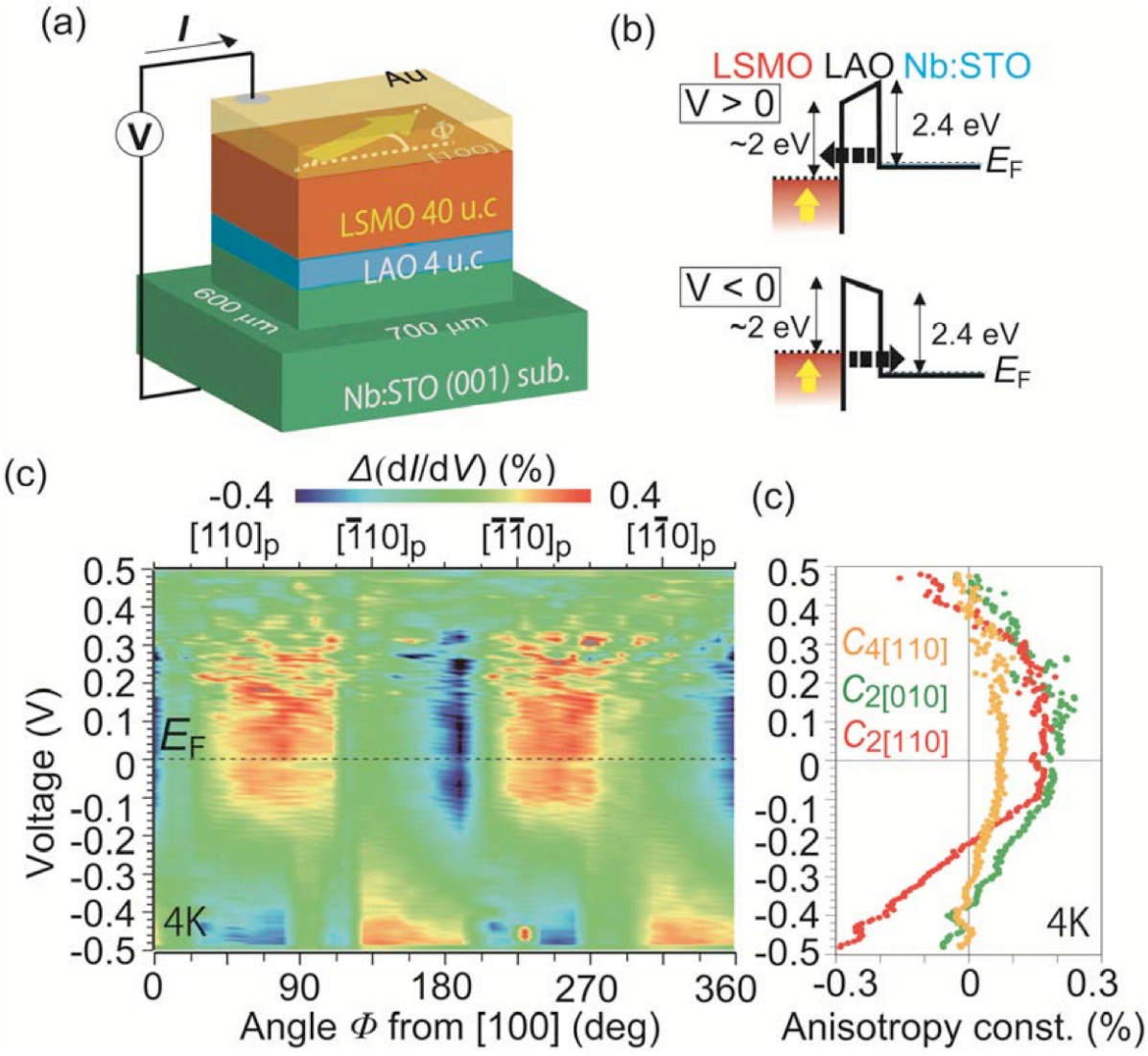

Fig. 1. (a) Device structure used for our measurements. (b) Conduction band (CB) profiles of the LSMO/ LAO/ Nb:STO tunneling diode under positive and negative bias voltages V. The solid and dotted lines represent the top of the CB and the Fermi level E_F. At positive (negative) V, the electrons tunnel from Nb:STO to LSMO (from LSMO to Nb:STO). (c) Color plots of $\Delta(dI/dV) = [dI/dV - \langle dI/dV \rangle_\Phi] / \langle dI/dV \rangle_\Phi \times 100(\%)$ as a function of Φ and V. Here, Φ is the magnetic-field angle from the $[100]_c$ axis in the counter-clockwise direction in the film plane, and $\langle dI/dV \rangle_\Phi$ is defined as averaged dI/dV over Φ at each V. All the data were measured at 4 K [5].

No. 15

Recent Trends in MTJ-Based Nonvolatile FPGA

D. Suzuki[1,3] and T. Hanyu[2,3]

[1] *Frontier Research Institute for Interdisciplinary Sciences, Tohoku Univ., Sendai, Japan*

[2] *Research Institute for Electrical Communication, Tohoku Univ., Sendai, Japan*

[3] *Center for Spintronics Research Network, Tohoku Univ., Sendai, Japan*

Email: daisuke.suzuki.e6@tohoku.ac.jp

In the smart internet of things (IoT) era, VLSI processors from low-end to high-end are indispensable to meet a wide variety of application requirements. A field programmable gate array (FPGA) is an effective way to implement such VLSI processors owing to its reconfigurable architecture. It is also expected that the FPGA is used as a hardware accelerator for brain-inspired computing and its higher energy efficiency compared to software-based method and graphic-processing unit (GPU) based one. However, because a large number of redundant components are required for the FPGA, standby power dissipation is a critical issue for the conventional SRAM-based FPGA. Therefore, like sensor node applications that operate under limited electricity such as an installed maintenance-free battery or energy harvesting is not suitable for the SRAM-based FPGA.

A nonvolatile FPGA (NV-FPGA), wherein all the data are stored in nonvolatile devices is one promising solution for the standby power problem. Because the circuit information is remained without power supply, standby power consumption is completely eliminated by utilizing power gating technique where power supply of idle circuit blocks are temporally cut off. Among several emerging nonvolatile devices, a magnetic tunnel junction (MTJ) device is a viable candidate given its 3-dimensional stacking capability, CMOS compatibility, and virtually unlimited endurance.

In this presentation, recent research trends in MTJ-based NV-FPGA [1-4] are presented. Especially, the advancements of a lookup table (LUT) circuit which is key component of the FPGA are presented.

References

[1] D. Suzuki et al., Symp. VLSI Circuits Dig. Tech. Papers, 172 (2015).
[2] D. Suzuki, et al., IEEE Trans. Magn. **50**, 3402104 (2014).
[3] D. Suzuki, et al., IET Electronics Lett. **53**, 456 (2017).
[4] D. Suzuki and T. Hanyu, Jpn. J. Appl. Phys. **57**, 04FE09 (2018).

No. 16

Anomalous Magnetic, Dielectric, and Optic Properties in Strained and Relaxed Rare-earth Iron Garnet Thin Films

Hiroyasu Yamahara[1], Sarker Md Shamim[1], Akihiro Katougi[1], Ryota Kikuchi[1], Munetoshi Seki[1], and Hitoshi Tabata[1]

[1] *University of Tokyo*, *Tokyo, Japan*

Email: yamahara@bioxide.t.u-tokyo.ac.jp

Rare-earth iron garnets (RIGs) are ferrimagnetic insulators whose chemical formula is $R_3Fe_5O_{12}$ (R : rare-earth elements). They have been commercially available for optical devices such as optical isolators since they show large magneto-optical effect. Among various RIGs, $Y_3Fe_5O_{12}$ (YIG) is widely studied for spinwave applications since the intrinsic Gilbert damping constant is exceptionally low as $\alpha = 10^{-5}$ in bulk. In this research, magnetic, dielectric, and optic properties of crystalline strained and relaxed RIG films are studied. YIG grown on $Gd_3Ga_5O_{12}$ (GGG) substrates has shape anisotropy with in-plane easy axis, while YIG on $Y_3Al_5O_{12}$ (YAG) are reported to shows strain-tunable magneto-crystalline anisotropy due to the strain-induced tetragonal distortion [1]. On the other hand, perpendicular magnetic anisotropy is reported in strained $Tm_3Fe_5O_{12}$ (TmIG) [2] and $Sm_3Fe_5O_{12}$ (SmIG) [3] thin films. When there is a lattice mismatch between RIG films and substrates, the crystal structure is epitaxially strained, therefore tetragonal structure is observed in the vicinity of interface. As the film thickness increase, misfit dislocation occurs at critical thickness t_c and lattice relaxation occurs. Around the surface, relaxed cubic structure is observed. At the vicinity of t_c, strain and relaxation co-exist, therefore strain-gradient structure is grown as illustrated in Figure 1. In the strain-gradient region, the asymmetric crystal structure is expected to generate electrical polarization known as flexoelectricity [4]. Since there are both magnetic moments and electrical polarization in the strain-gradient structure, multiferroic behaviors and magneto-electric correlation (ME-effect) are expected, which is useful for future application on spintronics devices. In this research, magnetic, dielectric and optical properties of SmIG thin films deposited on GGG substrates are discussed. The lattice mismatch between SmIG and GGG is 1.2%, so that the critical thickness t_c, where misfit dislocation occurs, is estimated to be 66 nm. When the thickness of SmIG is thicker than t_c, strain-gradient structure is expected between coherently strained tetragonal and relaxed cubic phases. SmIG films with various thickness are grown by pulsed laser deposition technique (PLD). The epitaxial relationship between films and substrates are confirmed by reciprocal space mapping (RSM) of X-ray diffraction (XRD). The magnetic property measurements are carried out by magnetic circular dichroism (MCD). In order to measure dielectric properties of SmIG films, interdigital electrodes (IDE) with 10 μm width and space are fabricated by photolithography and metal sputtering. Spectroscopic ellipsometry is measured for

optical property analysis.

Figure 2(a) shows thickness dependence of magnetic coercive field measured by MCD. When the thickness of SmIG film is around critical thickness, the magnetic coercivity shows maximum, which is because defects work as pinning sites of domain wall. Figure 2(b) shows thickness dependence of dielectric constant measured by using IDE. The dielectric constants are characterized from capacitance measured by impedance spectroscopy. In order to calibrate the effect of electrodes geometries and film thickness, calculation model reported by Farnell is applied [5]. As shown in Figure 2(b), dielectric constants shows maximum around critical thickness. The refractive indexes of SmIG films are also characterized by spectroscopic ellipsometry. We observe lower shift of light absorption edge for SmIG films that thickness is around critical thickness. These anomalous behaviors relate to dislocations and strain-gradient structures.

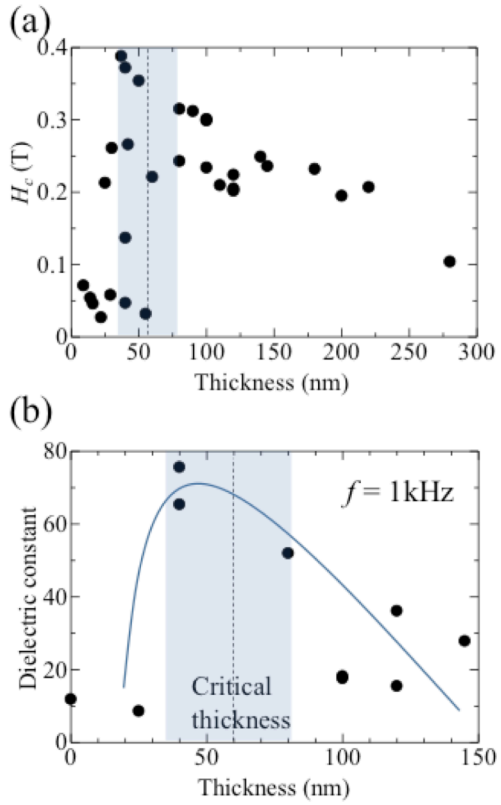

Figure 1. Schematic illustration of strained-tetragonal, strain-gradient, and relaxed cubic structures.

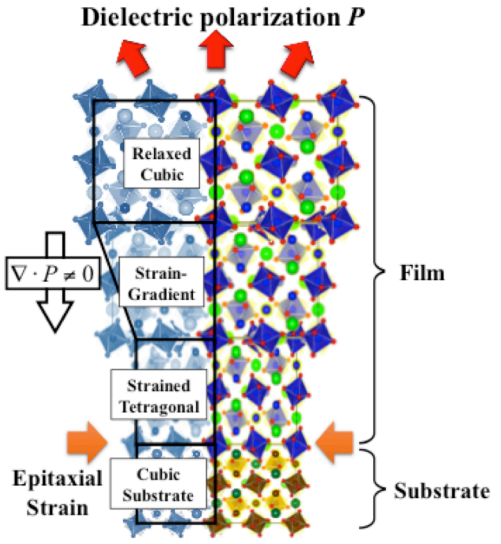

Figure 2. (a) Thickness dependence of coercive field measured by MCD. (b) Thickness dependence of dielectric constant measured by using interdigital electrodes.

References

[1] H. Wang et al., Phys. Rev. B, 89 134404 (2014).
[2] C. Tang et al., Phys. Rev. B, 94 140403 (2016).
[3] H. Yamahara et al., J. Mag. Mag. Mater., 323 3143 (2011).
[4] D. Lee et al., Phys. Rev. Lett. 107 057602 (2011).
[5] G. W. Farnell et al., IEEE. Trans. Sonics. Ultrason., SU-17, 188 (1970).

No. 17

Physical Implementation of Neuromorphic System

M. S. Sarker[1], H. Yamahara[1], M. Seki[1,2], Y. Hotta[3], and H. Tabata[1,2]

[1] *Department of Electrical Engineering and Information Systems, Graduate School of Engineering, University of Tokyo, Japan*

[2] *CSRN, Graduate School of Engineering, University of Tokyo*

[2] *Department of Electrical Materials and Engineering, University of Hyogo*

Email: yamahara@bioxide.t.u-tokyo.ac.jp

Neuromorphic system is an interdisciplinary research platform which incorporates the knowledge of biology, physics, mathematics, computer science and electronic engineering to design an artificial neural system. The artificial neural system is widely applied for vision system, head to eye system, auditory processors and autonomous robots, whose physical architecture and design principles are based on those of biological nervous system [1]. The accurate understanding of the morphology of individual neuron, its circuit application, overall architecture, incorporating the adaptability towards any environmental change and finally the learning and developments are the key aspects of the successful implementation of neuromorphic system. The hardware level implementation of the neuromorphic computing can be realized by oxide based memristor [2], threshold switch and transistor [3]. The fundamental part of the neuromorphic system design is to implement a system that can mimic the function of an individual neuron. Hotta et al. proposed a system named neuron like signal transducer (NST) based on stochastic resonance (SR) which can replicate the function of neuron [4]. In their report they used stochastic resonance between the weak neuron like signal and another signal with fixed amplitude, but wide range of frequency called Gaussian White Noise (GWN) to amplify and detect the weak biological signal. They used a comparator with a fixed threshold voltage in such a way that when the amplified signal crosses a predefined threshold then it will produce a neuron like spike signal. This predefined threshold of this NST limits it boundary to act like the biological neuron because predefined threshold makes its behavior more deterministic and can not react against the unpredictable and abrupt environmental change. To overcome this limitation a stochastically excitable threshold unit model has been reported [5] which uses multiple attractor. This is purely a simulation model which can mimic the stereopsis and binocular rivalry in the human visual cortex. The first target of this research is to implement this SR model of the attractor switching device using chip and characterize this neural system. The second stage is to adapt the multifunctional oxide-based memristor or active devices on the chip to design a complete neuromorphic system.

References

[1] Boddhu, S. K., Gallagher J. C., Appl. Comp. Intel. and Soft Computing, 1–21, 2012. [2] Maan, A. K.; Jayadevi, D. A.; James, A. P, IEEE Trans. on Neural Networks and Learning Systems. 99, 2016. [3] Zhou Y., Ramanathan S., Proc. of the IEEE. 103, 1289–1310, 2015. [4] Y. Hotta et al., Appl. Phys. Lett., 1, 088002, 2008. [5] N. Asakawa, Y. Hotta, T. Kanki, T.kawai, Phys. Rev. E 79, 021902, 2009.

No. 18

Thermal effect in magnetization dynamics induced by electric-field in a magnetic tunnel junction

S. Kanai,[1-3] Y. Nakatani,[4] F. Matsukura,[1-3,5,7] and H. Ohno[1-3,5-6]

[1]Laboratory for Nanoelectronics and Spintronics, Research Institute of Electrical Communication, Tohoku University, *Sendai, Japan*

[2]Center for Spintronics Integrated Systems, Tohoku University, *Sendai, Japan*

[3]Center for Spintronics Research Network, Tohoku University, *Sendai, Japan*

[4]University of Electro-Communications, *Tokyo, Japan*

[5]Center for Innovative Integrated Electronic Systems, Tohoku University, *Sendai, Japan*

[6]Center for Science and Innovation in Spintronics (Core Research Cluster), Tohoku University, *Sendai, Japan*

[7]WPI-Advanced Institute for Materials Research, Tohoku University, *Sendai, Japan*

Email: sct273@riec.tohoku.ac.jp

Electric-field induced magnetization switching was demonstrated in nanoscale magnetic tunnel junctions (MTJs). While clear oscillations in the switching probability were observed [1, 2], their amplitude decays within 5 periods, suggesting 10 times larger thermal agitation in magnetization dynamics expected from nucleation volume and damping constant. In this work, we measure magnetization dynamics in an MTJ by measuring transmitted voltage to elucidate the origin of this inconsistency.

An 80-nm-diameter MTJ with CoFeB (0.9 nm)/MgO/CoFeB (1.8 nm) is fabricated by sputtering and electron beam lithography. The CoFeB layers have perpendicular easy axis, and the 1.8-nm (0.9-nm) CoFeB layer is free (reference) layer. We induce the free layer magnetization precession about the in-plane component of external magnetic field by applying voltage pulses with ns duration. The magnetization dynamics is monitored as the transmitted voltage using high-speed oscilloscope, which reflects the perpendicular magnetization component in the free layer through the tunnel magnetoresistance effect.

The single-shot measured magnetization precession manifests itself as a clear oscillation with a 2 ns oscillatory period in the transmitted voltage. The amplitude of oscillation does not show significant decay up to ~6 periods, while the phase of the oscillation shifts randomly with time. It is clarified that oscillation frequency depends on its amplitude. Taking this phase-amplitude coupling into account, the decays of the averaged oscillation in transmitted voltage and switching probability within ~5 periods [1,2] are explained by thermal effect expected from nucleation volume and damping constant.

This work was supported in part by R&D Project for ICT Key Technology of MEXT, and the Cooperative Research Project of RIEC, Tohoku University.

References

[1] Y. Shiota *et al*., Nature Mat. **11**, 39 (2012).
[2] S. Kanai *et al*., Appl. Phys. Lett. **101**, 122403 (2012).

No. 19

Magnetism of Eu-doped GaN nanostructures by spinodal decompositions

A. Masago[1], H. Shinya[21], T. Fukushima[31], K. Sato[41], and H. Katayama-Yoshida[5]

[1] *Center for Spintronics Research Network, Graduate School of Engineering Science, Osaka University, Toyonaka, Japan*

[2] *Graduate School of Engineering, Yokohama National University, Yokohama, Japan*

[3] *Institute for NanoScience and Design, Osaka University, Suita, Japan*

[4] *Graduate School of Engineering, Osaka University, Suita Japan*

[5] *Center for Spintronics Research Network, Graduate School of Engineering, The University of Tokyo, Bunkyo-ku, Japan*

Email: masago@mp.es.osaka-u.ac.jp

Eu-doped GaN is renowned for red light emitting diodes, whereas it is interesting as a magnetic material. Some reported that Eu-doped GaN shows a ferromagnetic hysteresis in the magnetization curves against external fields, and others reported non-hysteretic sigmoidal curves. Meanwhile, it was reported that ErGaSb, which is a similar compound to Eu-doped GaN, exhibits nanostructures that are induced by spinodal decomposition.

In the previous study, we investigated that the mixing energy of EuN and GaN using Akai-KKR, which is based on the Korringa-Kohn-Rostoker method with the coherent potential approximation. [1] The mixing energy profile in Eu-doped GaN formed a convex upward arc; therefore, it is expected that Eu-doped GaN can also form nanostructures induced by spinodal decomposition. [2] The chemical pair interaction, which was calculated using the generalized perturbation method, also indicated an attractive trend between Eu ions in the zincblende GaN matrix. Using this chemical pair interaction, we obtained internal nanostructures or internal clusters of EuN depending on the annealing temperature, number of annealing steps, and Eu ion concentration. We proposed two phases that are called Dairiseki and Konbu phases. [1] The former phase occurs spontaneously and involves nano-dots, whereas the latter phase is artificially generated as to have nano-rods.

Here, we computationally generated two Dairiseki phases: one was generated by Monte-Carlo simulations with 10,000 (10k) Monte-Carlo steps, and the other was done with 1,000,000 (1M) steps. As shown in Fig.1 (left and middle), larger internal nanostructures are growing with the larger annealing steps. They were simulated with a 20×20×20 zincblende GaN supercell, where Eu ions located at Ga-sites on the lattice points, and the scaled temperature of $k_BT/|V_{01}|$ was set to 0.5, which corresponds to 428 K, and V_{01} indicates the chemical pair interaction between the nearest neighbor pair of Eu ions. The phase is generated using a crystal growth method: the three dimensional diffusion of impurities or dopants is allowed. An artificial phase, the Konbu phase, is

generated by a method: the two dimensional diffusion is allowed on each surface of the layer-by-layer crystal growth.

In this study we examine magnetization of the two Dairiseki phases by the Mote-Carlo method, where the parameters were calculated by Liechtenstein's formula. [3] Figure 1 (right) denotes the magnetization versus external field when the samples were generated with 10k Monte-Carlo steps (red boxes) and 1M steps (blue circles). The Dairiseki phase with 10k steps exhibits a paramagnetic behavior, because magnetic moments can move to the stable state over the barrier due to thermal fluctuation, but they hardly go back to the meta-stable state. According to statistical thermodynamics, some meta-stable spin states can persist, and the population difference between the two states contributes to magnetization.

The phase with 1M Monte-Carlo steps exhibits a hysteresis curve that is indicative of superparamagnetism. Because thermal fluctuation is small at this temperature, it hardly inverts spins against the barrier due to the magnetic pair interactions within the nanostructures. The number of magnetic impurities per nanostructure is proportional to the energy barrier height; therefore, the phase with larger internal nanostructures exhibits the larger hysteresis. These simulation results suggest that the different experimental results are due to the annealing time of these samples.

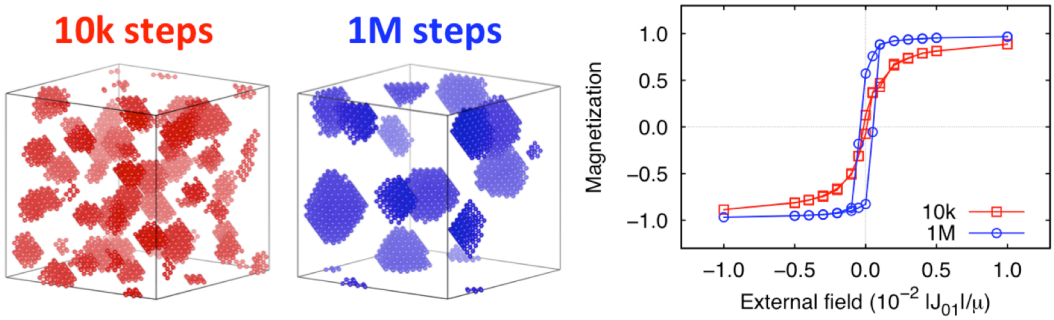

Fig.1: Virtual samples of Eu-doped GaN and their magnetization curves on external field. The left and middle figures indicate Dairiseki phases generated by Monte-Carlo simulations with 10k and 1M annealing steps, respectively. Particles denote Eu ions, whereas Ga and N ions are omitted. The right figure indicates their magnetization: red boxes and blue circles indicate magnetization of the samples generated with the 10k and 1M annealing steps, respectively. The magnetization is normalized so as to become 1 when all spins are parallel.

References

[1] H. Akai, J. Phys. Soc. Jpn. **51**, 468 (1982), http://kkr.issp.u-tokyo.ac.jp/jp/

[2] AM et 1al., Jpn. J. Appl. Phys. **55**, 070302 (2016).

[3] AM et al., submitted.

No. 20

Resistively-detected NMR in a quantum point contact in a low magnetic field

A. Noorhidayati[1], M. H. Fauzi[2,3], S. Maeda[1], K. Sato[1], K. Nagase[1], Y. Hirayama[1,2,3]

[1] *Department of Physics Tohoku University, Sendai 980-8579, Japan*

[2] *CSRN Tohoku University, Sendai 980-8577, Japan*

[3] *CSIS (Core Research Cluster) Tohoku University, Sendai 980-8577, Japan*

Email: noorhidayati.annisa.s3@dc.tohoku.ac.jp

Quantum point contact (QPC) can be used to electrically generate and probe the nuclear spin polarization [1-4]. The detection technique relies on the hyperfine coupling inducing a change in the QPC potential barrier. Here, we report RD-NMR measurement of ^{75}As nuclei in GaAs based QPC in quantum Hall breakdown regime in a relatively moderate to low magnetic field. We fabricated QPCs on both high-mobility GaAs (μ = 147 m^2 Vs at $n_s = 1.8 \times 10^{15}$ m^{-2}) and low-mobility (μ = 28 m^2 Vs at $n_s = 1.8 \times 10^{15}$ m^{-2}) AlGaAs/GaAs quantum wells.

It is important to find a suitable condition to perform RD-NMR in low magnetic field regime to tackle an interesting class of problem such as an anomalous conductance [2] observed in this regime. We approach low magnetic field regime in two different scenarios: (1) With the simplest possible case within the lowest Landau level (ν_{bulk}, ν_{qpc} = 2,1) by tuning back-gate voltage (V_{BG}) and split-gate voltage (V_{SG}); (2) Operating the NMR detection at high Landau levels. Using low mobility wafer we obtain RD-NMR signal down to 3T while using high-mobility wafer we manage to push detection limitation down to 1.25T (0.98T) for first (second) scenario.

References

[1] K. R. Wald *et al.*, Phys. Rev. Lett., **73**, 1011 (1994).

[2] M. Kawamura *et al.*, Phys. Rev. Lett., **115**, 036601 (2015).

[3] M. H. Fauzi *et al*., Phys. Rev. B 95, 201404(R) (2017).

[4] M. H. Fauzi *et. al.*, Phys. Rev. B **97**, 201412(R) (2018).

No. 21

Shape magnetic anisotropy from spin density approach

T. Oda[1, 2, 3], I. Pardede[2], T. Kanagawa[2], D. Yoshikawa[2], N. Ikhsan[2], and M. Obata[1, 2]

[1] *Institute of Science and Engineering, Kanazawa University, Kanazawa, Japan*

[2] *Graduate School of Natural Science and Technology, Kanazawa University, Kanazawa, Japan*

[3] *Center for Spintronics Research Network (CSRN), Osaka University, Toyonaka, Japan*

Email: oda@cphys.s.kanazawa-u.ac.jp

Magnetic anisotropy at surface/interface plays an important role of magnetic properties in magnetic or spintronic devices of nanoscale. The contribution of magnetic dipole-dipole couplings among electron spins cannot be neglected as well as that of spin-orbit couplings. Recently, complicated stackings of ferromagnetic/antiferromagnetic materials or junctions between different kinds of magnet are focused in the materials for memory or sensor, or for emerging new phenomena [1, 2]. In these contexts, we have implemented a computational method for estimating a magnetic anisotropy originating from the spin-orbit couplings in slabs. To evaluate the total magnetic anisotropy more precisely in slabs, we have also developed a new computational method for the magnetic dipole couplings in slabs [3]. We have applied it to a ferromagnetic slab with multi atomic layers to capture the usefulness of the method and to an antiferromagnetic slab showing a perpendicular contribution to the anisotropy from magnetic dipole couplings [4].

The new approach developed enables us to estimate the magnetic dipole energy of slab materials using a spin density obtained from a density functional approach, such as, based on density functional theory. In our implementation, we employed an ultrasoft-pseudopotential planewave-basis electronic structure calculation method. The magnetic anisotropy energy from magnetic dipole interaction (shape magnetic anisotropy energy) can be estimated accurately with a moderate computational cost for slabs. In a demonstration of ferromagnetic slab with Fe/MgO interfaces, the quadrupole component of atomic spin density suppresses the in-plane magnetic anisotropy energy, which results in an increase of perpendicular total magnetic anisotropy energy. In another demonstration of antiferromagnetic MnPt slab, which has a perpendicular favor originating from the crystalline magnetic dipole interaction, a surface effect of the Mn edge appears as an enhancement.

References

[1] S. Fukami et al., Nat. Mat. **15**, 535 (2016).

[2] T. Nozaki et al., Appl. Phys. Express **10**, 073003 (2017).

[3] T. Oda and M. Obata, J. Phys. Soc. Jpn. **87**, 064803 (2018).

[4] T. Oda et al., IEEE Trans. Magn. **55**, (2018), DOI: 10.1109/TMAG.2018.2868843.

No. 22

Quantum confinement phenomena in transition metal dichalcogenides

Mohammad Saeed Bahramy

Department of Applied Physics, The University of Tokyo, Tokyo 113-8656, Japan
Email: bahramy@ap.t.u-tokyo.ac.jp

Gate-voltage control of surface and interface charge carrier densities not only lies at the heart of modern microelectronic devices such as the ubiquitous semiconductor transistor, but also provides a mechanism for stabilizing new physical regimes. The injection of large sheet carrier densities, utilizing approaches such as ionic liquid gating has further established the potential to obtain gate-voltage control over the collective states of materials. Transition metal dichalcogenides have particularly proven to be ideal systems for realizing a variety of exotic quantum phenomena via electrical gating. In this presentation, I will discuss a number of novel phenomena emerging from quantum confinement of carriers at the surface of TMD's. In particular, for semi-metallic TMD PtSe2, I will show how the presence of both electron- and hole-like bulk carriers causes the near-surface band bending potential to develop an unusual non-monotonic form (see Figure 1), with spatially-segregated electron accumulation and hole accumulation regions, which in turn amplifies the induced spin splitting [1].

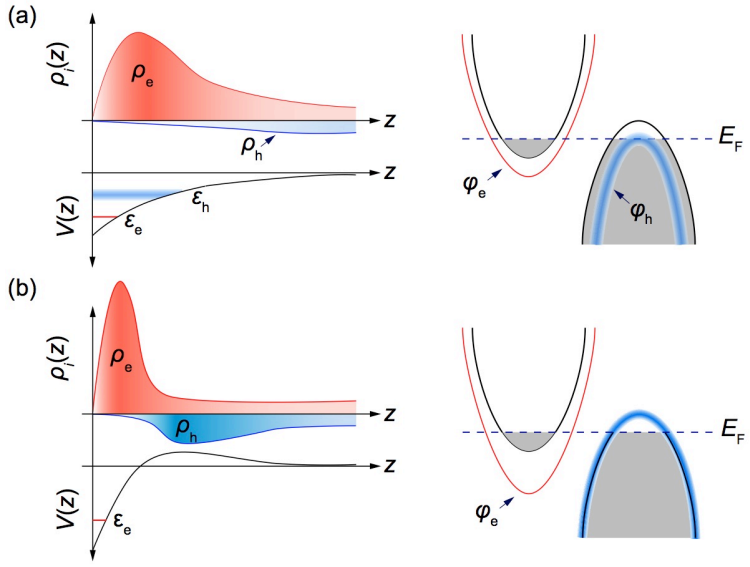

Figure 1. Schematic illustration of quantum confinement of surface states in a compensated semimetal, considering (a) a conventional band bending potential and (b) a real potential satisfying the Poisson equation for such a double-carrier system.

[1] O. J. Clark, F. Mazzola, J. Feng, V. Sunko, I. Markovic, L. Bawden, T. K. Kim, P. D. C. King, and M. S. Bahramy, submitted.

No. 23

Unveiling Origin of Ferromagnetism in Fe-Doped Ferromagnetic Semiconductor by Synchrotron Radiation Spectroscopy

M. Kobayashi[1,2,3,4], L. D. Anh[1,2,3], P. N. Hai[1,5], H. Kiuchi[4], H. Niwa[4], J. Miyawaki[6], Y. Harada[6], T. Schmitt[2], A. Fujimori[7], V. N. Strocov[2], M. Oshima[4], and M. Tanaka[1,3]

[1]*Center for Spintronics Research Network (CSRN), The University of Tokyo, Japan*

[2] *Swiss Light Source, Paul Scherrer Institut, Switzerland*

[3]*Department of Electrical Engineering and Information Systems, The University of Tokyo, Japan*

[4]*Department of Applied Chemistry, The University of Tokyo, Japan*

[5]*Department of Electrical and Electronic Engineering, Tokyo Institute of Technology, Japan*

[6]*Institute for Solid State Physics, The University of Tokyo, Japan*

[7]*Department of Physics, The University of Tokyo, Japan*

Email: masaki.kobayashi@ee.t.u-tokyo.ac.jp

Ferromagnetic semiconductor (FMS), which has both the semiconducting and ferromagnetic properties, is one of the most important fundamental subjects in spintronics due to its compatibility with the semiconductor technology. Prototypical Mn-doped FMSs such as (Ga,Mn)As [1] and (In,Mn)As [2] show ferromagnetism originating magnetic interaction between magnetic Mn ions through spin of carriers. This ferromagnetism is called carrier-induced ferromagnetism that enables us to manipulate both the charge and spin degrees of freedom. However, the Curie temperature (T_C) of the Mn-doped III-V FMSs is lower than room temperature (T_C < 200 K) and the Mn-doped FMSs are basically *p*-type (there is no *n*-type) because the Mn ions act as acceptors. To make these FMSs useful for practical applications, we have to solve these problems.

Recently, new Fe-doped narrow-gap III-V-based FMSs were successfully grown by molecular beam epitaxy. Among them, (In,Fe)As was found to be an *n*-type FMS with electron-induced ferromagnetism [3]. Although this is a narrow-gap semiconductor, (In,Fe)As has relatively high T_C (~120 K at mzximum so far). Since coped Be ions act as double donors in (In,Fe)As when grown at low temperature (~240 ^oC), one can independently control the magnetic moment given by Fe and carrier concentration by Be doping [3]. Subsequently, other Fe-doepd narrow-gap III-V-based FMSs *p*-type (Ga,Fe)Sb [4], insulating (Al,Fe)Sb [5], and *n*-type (In,Fe)Sb [6,7] have been successfully grown. Surprisingly, (Ga,Fe)Sb and (In,Fe)Sb show ferromagnetism with T_C above room temperature. Therefore, Fe-doped FMSs will open up new possibilities and opportunities both in fundamental research and device applications.

To understand the physical properties the carrier-induced ferromagnetism and design the spintronic devices using *n*-type FMSs, it is indispensable to reveal the band structure. Here, we have studied the valence-band structure and the local electronic structure of the Fe ions in Be doped $In_{0.95}Fe_{0.05}As$ (Be concentration: 2×10^{19} cm^{-3}),

using soft X-ray angle-resolved photoemission spectroscopy (SX-ARPES) and soft X-ray resonant inelastic X-ray scattering (SX-RIXS), respectively, for unveiling the origin of the carrier-induced ferromagnetism.

Figure 1 shows the band dispersion along the Γ-K-X symmetry line taken at $h\nu = 908$ eV. In addition to the light-hole (LH) and split-off (SO) bands, the small but definitive electron conduction band crossing the Fermi level (E_F) exists around the Γ point. This observation is consistent with the *n*-type nature of (In,Fe)As and indicates that its conduction band crosses E_F. The resonant ARPES spectra at Fe L_3 edge clearly shows the Fe 3*d*-derived impurity band located near the conduction band minimum. As to the local electronic structure of Fe ions, we have conducted the SX-RIXS measurements. The Fe L_3 RIXS spectra of (In,Fe)As consist of the fluorescence and Raman components and the line shapes of the spectra are broadened like Fe metal. This observation indicates that the Fe 3*d* state is energetically broadened through hybridization with the ligand band. Based on these findings, we conclude that the 'conduction band' (Zener *s*,*p*-*d* exchange) model based on itinerant carriers is appropriate for explaining the carrier-induced ferromagnetism in Be-doped (In,Fe)As.

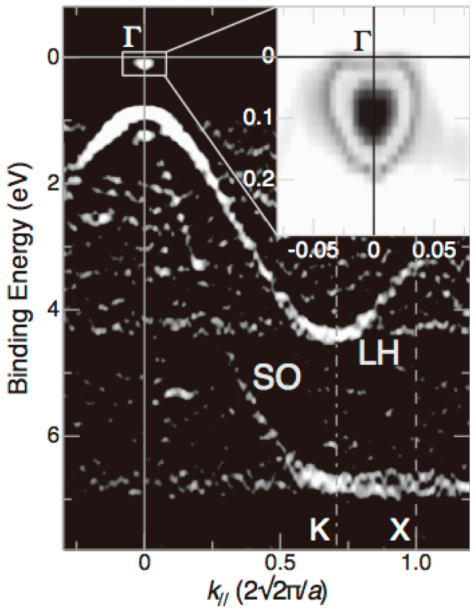

FIG. 1. Band dispersion along the Γ-K-X line of Be-doped $In_{0.95}Fe_{0.05}As$. Here, the Be concentration is about 2×10^{19} cm^{-3}. The inset is an enlarged figure around the Γ point. LH and SO denote the light-hole and split-off bands.

References

[1] H. Ohno *et al*., Appl. Phys. Lett. **69**, 363 (1996).
[2] H. Munekata *et al*., Appl. Phys. Lett. **63**, 2929 (1993).
[3] P. N. Hai *et al*., Appl. Phys. Lett. **101**, 182403; *ibid*, 252410 (2012).
[4] N. T. Tu *et al*., Appl. Phys. Lett. **105**, 132402 (2014).
[5] L. D. Anh *et al*., Appl. Phys. Lett. **107**, 232405 (2015).
[6] A. V. Kudrin *et al*., J. Appl. Phys. **122**, 183901 (2017).
[7] N. T. Tu *et al*., Appl. Phys. Exp. **11**, 063005 (2018).

No. 24

Giant magnetoresistance in phthalocyanine molecular mixed crystals and binary semimetal

N.Hanasaki, H.Murakawa, K.Yokoi, R.Ishii, M.Ikeda, and H.Sakai
Dept. of Physics, Osaka University, Osaka 560-0043, Japan
Email: hanasaki@phys.sci.osaka-u.ac.jp

The giant magnetoresistance is a fundamental phenomenon originating from the interplay between electricity and magnetism, and is applied to a wide variety of instruments. This effect is a central research topic in the material science. We observed the giant magnetoresistance in the molecular conductor $TPP[Fe(Pc)(CN)_2]_2$ (Pc = phthalocyanine and TPP＝tetraphenylphosphonium). The intersite Coulomb interaction causes the charge order of π-conduction electron, which the antiferromagnetic order of d local moments also stabilizes. In the magnetic field, since the local moments are aligned by the magnetic field, the stability of the charge order is reduced, leading to the giant magnetoresistance. Since the interaction between the π-conduction electron and d local moment is ferromagnetic ($|J/k_B|$>500K), the mechanism of this giant magnetoresistance effect is similar to that observed in the manganese oxides. In contrast to the oxides, we can control the density and the moment size of the localized spins. We investigated the magnetoresistance in various local-moment densities. In the lower local moment density, the stability of the antiferromagnetic order is reduced, leading to the enhancement of the sensitivity to the magnetic field. In the low spin density of 33%, the resistivity in 9T is three orders of magnitude smaller than the zero-field resistivity.

The binary semimetals are also promising materials for the giant magnetoresistance effect. We have observed an extremely large magnetoresistance exceeding 1.9 million at 1.7K at 40T in $NbAs_2$. This magnetoresistive behavior is quantitatively reproduced by a semiclassical two-carrier model in which the significant enhancement of magnetoresistance is attributed to the almost full compensation of the hole and electron densities ($0.994 < n_h/n_e < 0.999$) as well as the high mobility ($>6 \times 10^5$ $cm^2/V \cdot s$). Our results indicate that binary semimetals with higher carrier densities have a great potential for exhibiting a further divergent increase in magnetoresistance merely through an improvement in crystal quality.

References

[1] R. Ishii, H.Murakawa, M.Nishi, M.Matsuda, H.Sakai, and N.Hanasaki, J.Crystal Growth **487**, 92 (2018).
[2] K.Yokoi, M.Murakawa, M.Komada, T.Kida, M.Hagiwara, H.Sakai, and N.Hanasaki, Phys.Rev.Materials **2**, 024203 (2018).

No. 25

High S_{21} property in heat-driven magnetic tunnel junction

°Y. Yamada[1], M. Goto[1,4], T. Yamane[2], N. Degawa[2], T. Suzuki[2], A. Shimura[2], S. Aoki[2], J. Urabe[2], S. Hara[2], S. Miwa[1,3,4]and Y. Suzuki[1,4]

Osaka Univ. [1], TDK [2], Univ. of Tokyo [3], CSRN-Osaka [4]

E-mail: yamada@ spin.mp.es.osaka-u.a.jp

Various radio-frequency (RF) applications using a Magnetic tunnel junction (MTJ) have been developed, for example, spin-torque oscillator, spin-torque diode. In addition to these devices, MTJ can be used as amplifier of RF signals. Input RF signal is amplified by ferromagnetic resonance (FMR) with a direct current applying to MTJ. The RF reflected signal from MTJ was tried to be amplified using FMR excited by spin-transfer torque, RF external magnetic field [1-2]. Recently, it is reported that the amplification is succeeded by using anisotropy change [3].

In this study, we demonstrate the high S_{21} value using MTJ and its physical mechanism. To excite the FMR efficiently, we change the anisotropy energy by Joule-heating. Figure 1 shows the perpendicular magnetic anisotropy (PMA) change as a function of applying voltage. We observed the parabolic anisotropy change. This means that PMA was changed by Joule-heating. We also observed large anisotropy change 847 μJ/m^{2}V. Figure 2 shows the spectrum at highest S_{21} value when we applied magnetic field and dc current to MTJ. The S_{21} > 0 dB was observed, which means that the input signal was amplified.

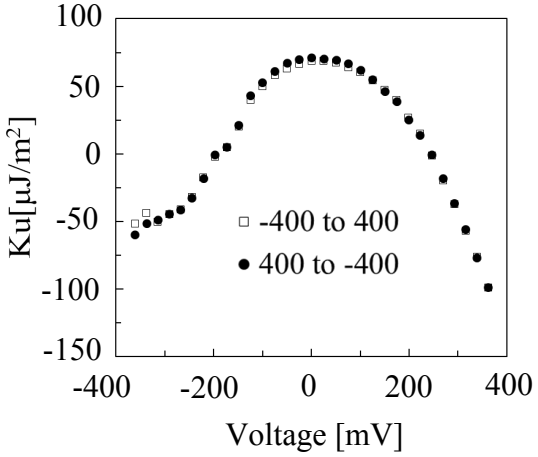

Fig.1: Perpendicular magnetic anisotropy changed by voltage

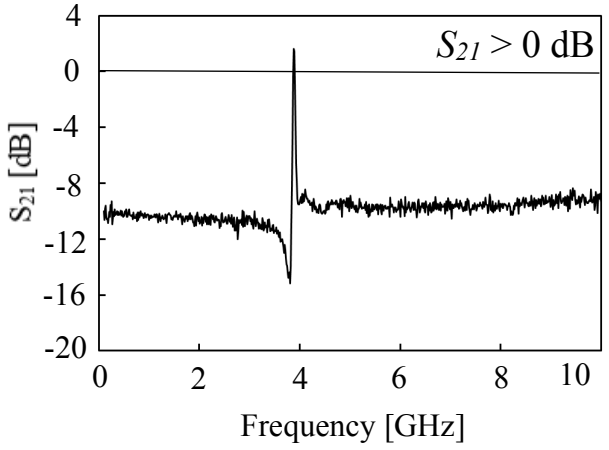

Fig.2: The S_{21} spectrum at its highest

References

[1] Xue et al., Appl. Phys. Lett. **99,** 022505 (2011)

[2] K. Konishi et al., Appl. Phys. Lett. **102,** 162409 (2013)

[3]M.Goto et al., Nat. Nanotechnol, accepted

No. 26

Brownian motion of skyrmions: -their normal and gyro diffusion coefficients-

S. Miki[1], Y. Jibiki[1], J. Cho[3], E. Tamura[1], M. Goto[1, 2], Y. Suzuki[1, 2]

[1]*Graduate. School of Engineering Science, Osaka University, Japan*

[2]*Center for Spintronics Network (CSRN), Osaka University, Japan*

[3]*Spin Convergence Research Team, KRISS, Korea*

Email: miki@spin.mp.es.osaka-u.ac.jp

The topologically protected magnetic spin configurations known as Skyrmions offer promising applications due to their stability, mobility, and localization [1]. As its peculiar application, thermally induced skyrmion dynamics can be used for unconventional computing i.e. the probabilistic computing [2,3] and the Brownian computing [4]. In this work, we study the thermal motion of skyrmions which depends on their size and profile, taking into account the gyromagnetic coupling effects and the tensor mass of skyrmions in same footing.

A skyrmion is characterized by its size and profile, that is, the skyrmion radius R, the domain wall width w, the skyrmion charge q and the helicity γ_{helicity} [5]. Skyrmion dynamics is accordingly characterized by these 4 parameters. The 2-dimentional Brownian motion can be described by the double-time correlation functions of the coordinates x and y, $\langle x(t)x(t')\rangle$, $\langle y(t)y(t')\rangle$ and $\langle y(t)x(t')\rangle$. These are obtained from the velocity-velocity correlations calculated from the generalized Thiele equation [1,6],

$$\langle v_x(t)v_x(t')\rangle = \langle v_y(t)v_y(t')\rangle = \frac{k_BT}{m} e^{-\frac{\alpha D}{m}|t-t'|} \cos\frac{G}{m}(t-t'), \tag{1}$$

$$\langle v_x(t)v_y(t')\rangle = -\langle v_y(t)v_x(t')\rangle = \frac{k_BT}{m} e^{-\frac{\alpha D}{m}|t-t'|} \sin\frac{G}{m}(t-t'), \tag{2}$$

where G, α, D and m are the gyrocoupling, the damping constant, the dissipation dyadic and the skyrmion effective mass [8], respectively. The gyrocoupling makes the skew velocity-velocity correlation $\langle v_x(t)v_y(t')\rangle$ sizable whose value is comparable to those of $\langle v_x(t)v_x(t')\rangle$ and $\langle v_y(t)v_y(t')\rangle$. The latter two correlation functions have been reported by several authors [1,7]. The gyrocoupling depends exclusively on G which is proportional to skyrmion charge q, and therefore independent of skyrmion sizes and profiles. On the other hand, the dissipation dyadic D depends on the ratio R/w as well as q.

The normal and gyro diffusion coefficients are also obtained from the Eqs. (1,2) after

integration with respect to t' with the initial condition $x(0)=y(0)=0$ (Fig. 1a, 1b),

$$D_{xx} \equiv \frac{\left\langle \left(x(t)\right)^2 \right\rangle}{2t} = \left\langle v_x(t)x(t) \right\rangle, \quad D_{yy} = \left\langle v_y(t)y(t) \right\rangle = D_{xx}, \tag{3}$$

$$D_{xy} \equiv \left\langle v_x(t)y(t) \right\rangle, \quad D_{yx} \equiv \left\langle v_y(t)x(t) \right\rangle = -D_{xy}. \tag{4}$$

From Eqs. (4), we obtain the xy correlation function and find $\left\langle x(t)y(t') \right\rangle \neq 0$ when $t \neq t'$, while $\left\langle x(t)y(t) \right\rangle = 0$ when $t = t'$ (Fig. 2). We will give further discussion on our results.

Acknowledgement; This research and development work was supported by the Ministry of Internal Affairs and Communications.

References

[1] C. Schütte, N. Nagaosa et al, Phys. Rev. B **90**, 174434 (2014)
[2] D. Pinna, J. Grollier et al, Phys. Rev. Applied **9**, 064018 (2018)
[3] J. Zázvorka, M. Kläui et al, arXiv:1805.05924 (2018)
[4] J. Lee, F. Pepper et al, Int Journ of Unconventional Computing **12**, 341-362 (2016)
[5] X.S. Wang, X.R. Wang et al, Commun. Phys. **1**, 31 (2018)
[6] A. Thiele, Phys. Rev. Lett. **30**, 230 (1973)
[7] J. Miltat, A. Thiaville et al, Phys. Rev. B **97**, 214426 (2018)
[8] R.Troncoso, A. Núñez, Ann Phys **351, 850** (2014)

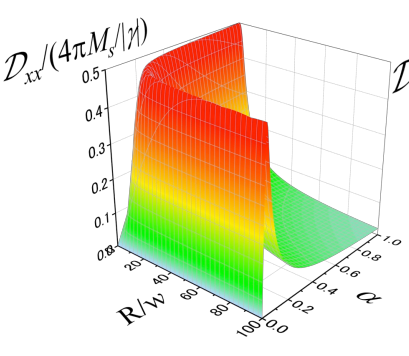

Fig. 1a Normal diffusion coefficient

$$D_{xx} = \frac{k_B T}{\alpha D} \frac{1}{1+\left(G/\alpha D\right)^2}$$

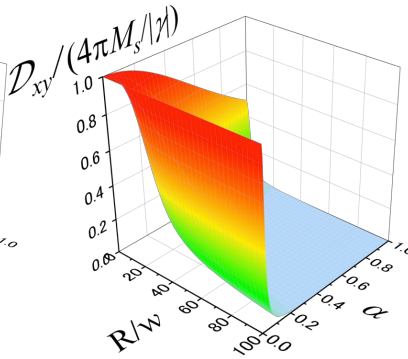

Fig. 1b Gyro diffusion coefficient

$$D_{xy} = \frac{k_B T}{\alpha D} \frac{G/\alpha D}{1+\left(G/\alpha D\right)^2}$$

$|\gamma|$ is gyro magnetic ratio,
and M_s is saturated magnetization

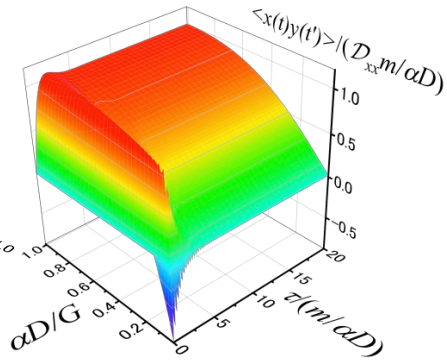

Fig. 2 yx-correlation function $\left\langle y(t')x(t) \right\rangle;\ \tau = t'-t$

No. 27

Computational Nano-Materials Design of $CsSnI_3$ Photovoltaic Solar Cells

H. Nagayama[1], H. Shinya[1,2], and K. Ohno[1]

[1] *Graduate School of Engineering, Yokohama National University, Yokohama.*

[2] *Center for Spintronics Research Network, Osaka University, Osaka.*

Email: nagayama-hiroshi-gm@ynu.jp

Recently, the perovskite-type semiconductors have attracted much attention as a light absorption layer of photovoltaic solar cells (PVSCs). The most famous perovskite-type PVSC is the organic-inorganic hybrid halide $CH_3NH_3PbI_3$ due to the high conversion efficiency (~22.1%) [1]. However, because CH_3NH_3 is degraded by light irradiation and Pb atom is harmful, we need to find the alternative materials. One of the candidates is $CsSnI_3$, where CH_3NH_3 and Pb are replaced with Cs and Sn, respectively.

In this study, we have performed the density functional theory calculations and investigated the electronic structures and structural stabilities. According to our results, the ordered defect compounds (ODCs) such as SnI_3 precipitate in the $CsSnI_3$ host material. Moreover, we found that the $CsSnI_3$ tends to separate into the ODC and $CsSnI_3$ phases by the spinodal and binodal decomposition. As a result, the recombination rate of the electron-hole pairs is suppressed, so that the conversion efficiency might increase [2].

Our calculations are based on the density functional theory. The electronic structures and the formation energies are calculated by the Vienna ab initio simulation package (VASP), on the basis of the projector augmented wave (PAW) method [3-5]. We calculated the mixing energies and phase diagrams by the Korringa-Kohn-Rostoker Green's function method with the coherent potential approximation (KKR-CPA) [6].

References

[1] http://www.nrel.gov/ncpv/

[2] T. Kishida and T. Nakase unpublished data.

[3] G. Kresse and J. Hafner, Phys. Rev. B 47, 558(R) (1993).

[4] G. Kresse and J. Furthmüller, Phys. Rev. B 54, 11169 (1996).

[5] G. Kresse and J. Furtfumüller, Comput. Mater. Sci. 6, 15 (1996).

[6] H. Akai, J. Phys. Soc. Jpn. 51, 468 (1982).

No. 28

Unexpected surface state of topological nodal-line semimetal

S. Souma [1,2]

[1] *Center for Spintronics Research Network (CSRN), Tohoku University, Sendai, Japan*

[2] *WPI-Advanced Institute of Materials Research (WPI-AIMR), Tohoku University, Sendai, Japan*

Email: s.souma@arpes.phys.tohoku.ac.jp

Topological semimetals (TSM) are recently becoming a leading platform for realizing exciting topological phases of matter. In contrast to conventional semimetals with a finite band overlap between valence band (VB) and conduction band (CB), topological semimetals are categorized by the band contacting nature between the VB and CB in the Brillouin zone; point-contact (Dirac/Weyl semimetals) or line contact (line-node semimetals; LNSMs). TSM shows a singularity of Berry curvature around such nodal electronic states, giving rise to various quantum phenomena like chiral anomaly, anomalous Hall effect, and large negative magnetoresistance. In this poster, we show our recent ARPES results on the candidates of such TSM's [1-3]. Figure 1a shows a quasi-two-dimensional Fermi surface hosting bulk nodal lines of HfSiS [2]. Most notably, we discovered an unexpected Dirac-like dispersion extending one-dimensionally in k space – the Dirac-node arc – near the bulk node at the zone diagonal as schematically depicted in Fig. 1b [2]. These Dirac states reside on the surface and could be related to hybridizations of bulk states, but currently we have no explanation for its origin. This discovery poses an intriguing challenge to the theoretical understanding of line-node semimetals. In this talk, we also present our data on various TMS and discuss a connection to the expected quantum phenomena.

This work has been done in collaboration with D. Takane, T. Nakamura, K. Nakayama, T. Takahasi, T. Sato, K. Yamauchi, T. Oguchi, K. Horiba, H. Kumigashira, K. Segawa, Z. Wang, and Y. Ando.

References

[1] S. Souma *et al*, Phys. Rev. B **93**, 161112R (2016).
[2] D. Takane *et al*., Phys. Rev. B **94**, 121108R (2016).
[3] D. Takane *et al*., npj Quantum Materials **3**, 1 (2018).

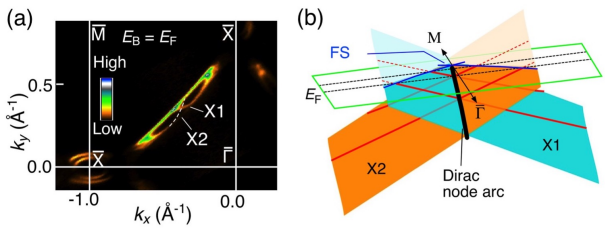

Fig. 1 (a) ARPES-intensity mapping at Fermi level of HfSiS. (b) Schematic band dispersion in 3D E-k space for the new surface states X1 and X2. Black line indicates the Dirac-node arc.